Laser cooling of cavitating bubbles for quantum technology applications

Amjad Aljaloud

Department of Physics and Astronomy

University of Leeds

A thesis submitted for the degree of

Doctor of Philosophy

5th Jul 2021

This thesis is dedicated to my parents who always believe in me. Without their endless love and encouragement I would never have been able to complete my graduate studies. I love you both and I appreciate everything that you have done for me.

Acknowledgements

Pursuing this PhD has been a truly life-changing experience for me, and it would not have been possible without Allah, who provides me with the strength to embark on this journey, and the encouragement and guidance I received from a large number of people.

I would like to express my sincere gratitude and thanks to my supervisor Dr. Almut Beige for her able guidance, keen interest and valuable suggestions in carrying out this piece of research work which finally resulted in the completion of this thesis. She has been incredibly supportive throughout my PhD journey, and particularly during the COVID-19 pandemic period.

I would like also to convey my sincere thanks to Prof. Jiannis Pachos, Dr. Sally Peyman and Dr. David Jennings for their continuous support and the confidence they gave me to keep going. I am particularly thankful for Prof. Apostolos Vourdas and Dr. Rob Purdy for agreeing to take time out of their schedules to be my examiners.

My sincere acknowledgement and gratitude are also extended to all my colleagues of the Department of Physics at University of Hail in Saudi Arabia for their continuous support and encouragement throughout my research.

Finally, I am especially grateful to my parents for their love and encouragement, without whom I would never have enjoyed so many opportunities. My two daughters Almas and Amal, my two sons Rakan and Tamim and my husband Turki, the real inspiration and supporting pillars, need no mention. Their understanding and inspiration persistently pushed me ahead to finish the work well in time.

Abstract

Since its invention almost 50 years ago, laser cooling has become a very powerful technique for cooling single atomic particles to very low temperatures. Laser cooling has been an essential tool in many fundamental tests of quantum physics but also enabled a wide range of quantum technologies. Unfortunately, laser cooling does not work for macroscopic systems, since these have a continuum of phonon modes and cooling all of them simultaneously becomes impossible without also inducing heating processes. Some tricks have been found to transfer atomic gases to very low temperatures, as needed for example for the preparation of Bose-Einstein condensates. But these techniques, like evaporative cooling have many disadvantages, and require for example the removal of atoms from the trap.

Here we have a closer look at alternative techniques for cooling atomic gases to very low temperatures. We propose to cool only a single collective mode of the gas but then use energy transfer processes due to thermalisation to lower the temperature of the remaining modes. As we shall see below,these thermalisation processes occur naturally in cavitating bubbles. Moreover, bubble collapse phases can be used to establish a collective phonon mode, which can be cooled very efficiently.

In summary, this thesis discusses the collective laser cooling of an atomic gas in cavitating bubbles. Moreover, we show that these might have applications as quantum heat exchangers, which cool a surrounding liquid for micro and nano technology applications. We hope that our work helps to initiate novel quantum optics experiments with cavitating bubbles.

Abbreviations

k_{B}	Boltzmann's constant
$k_B T$	Thermal energy
$\hbar$	Planck's constant
Tr	The trace operator

Thesis publications

1) "A quantum heat exchanger for nanotechnology" Amjad Aljaloud , Sally A. Peyman, and Almut Beige Entropy 22.4 (2020): 379.

2) "Laser cooling of indistinguishable particles in cavitating bubbles" Amjad Aljaloud and Almut Beige (in preparation).

Contents

List of Figures

Chapter 1

Introduction

This thesis combines three different topics, namely, laser cooling of atomic systems, the thermodynamics of harmonic oscillators and sonoluminescence. Our aim is to address a radically new model, integrating the quantum optics systems with the thermodynamics framework. More concretely, the main result of this thesis is a novel laser cooling scheme for an atomic gas which takes advantage of atom-phonon interactions as well as thermodynamic equilibrium formation. The main idea in our scheme is that, traditional laser cooling is a one step process. It only has a cooling phase. However, cooling processes in classical thermodynamics have usually many steps, like the Carnot cycle. Here we combine ideas from classical thermodynamics and laser cooling and design a two step process (intermittent cooling and thermalisation stages) to cool an atomic gas. This means, we overcome some limitations of laser cooling of many atoms which cannot be done in one step.

To implement the two-stage process we take advantage of the phenomenon of sonoluminescence. The two-stage process of the many-body cooling in an optical cavity has many similarities with the lifecycle of the single bubble, which is shaped by thermalisation and atom cavity phonon interactions (Kim *et al.* (2018)).

The principal result of this thesis is the design of a novel cooling scheme for many particles inside cavitating bubbles. As we shall see below, we use the bubble collapse phase, when the atoms inside the bubble are strongly confined, to implement laser cooling. However, between collapse phases, the atoms evolve adiabatically and energy is exchanged according to the laws of thermodynamics.

We also studied the single atom as a background to many body interactions in a similar setup. We give an overview over the whole thesis in the next sections. In what follows, we first introduce laser cooling of atomic systems in section 1.1. The cavity-mediated laser cooling will be described in a more intuitive way in Section 1.2. The quantum sonoluminescence is outlined in Section 1.3. Moreover, the structure of the thesis is highlighted in section 1.4.

1.1 Laser cooling of atomic systems

For quite some time laser cooling of atomic systems has been interesting. The technology is very important and allows the atomic system to cool to very low temperatures. A laser-cooled single atom is an outstanding way of realising a system that can be described by the theoretical models in quantum optics (Neuhauser *et al.* (1978)). This is the preferred subject for ultra-high precision testing, which tests the foundations of quantum physics and of a single trapped and laser cooled atom. From quantum metrology to quantum computing, laser cooling applications vary.

Since its discovery in Hänsch & Schawlow (1975); Wineland & Dehmelt (1975), laser cooling of individually trapped atomic particles has become a standard technique in quantum optics laboratories world-wide (Neuhauser *et al.* (1978); Wineland *et al.* (1978)). Rapidly oscillating electric fields can be used to strongly confine charged particles, like single ions, for relatively large amounts of time. Moreover, laser trapping provides unique means to control the dynamics of neutral particles, like neutral atoms (Chu (1998); Phillips (1998)). To cool single atomic particles, laser fields are applied which remove vibrational energy at high enough rates to transfer them down to near absolute-zero temperatures (Leibfried *et al.* (2003a)). Nowadays, ion traps are used to perform a wide range of high-precision quantum optics experiments. For example, individually trapped ions are at the heart of devices with applications in quantum technology, like atomic and optical clocks (Flannigan *et al.* (2005); Ludlow *et al.* (2015)), quantum computers (Debnath *et al.* (2016); Leibfried *et al.* (2003b); Schmidt-Kaler *et al.* (2003); Stephenson *et al.* (2020)), quantum simulators (Barreiro *et al.* (2011); Porras & Cirac (2004))and electric and magnetic field sensors (Maiwald *et al.* (2009)).

1.2 Cavity-mediated laser cooling

Laser cooling is powerful but not very effective at cooling multiple particles at the same time (Maunz *et al.* (2004)). However, cooling different types of body systems such as atomic gasses or condensates is essential for gaining insight into ultracold atomic physics. For the study and understanding of quantum phenomena like quantum phase transition, Bose-Einstein condensation, quantum magnetism, or bosonic superfluidity, ultracold atom experiments are important (Madison (2013)). Such experiments require a correct technology that would produce very low temperatures and relatively quick cooling.

As a solution for the effective cooling of a multi-body system, an atomic system has been coupled with quantised vibrational mode in an optical cavity. First signs of successful laser cooling mediated by a cavity in an experiment have been found by Vigneron (1995). Later on, it was demonstrated repeatedly that cooling processes could be greatly improved for single and multi-part system by adding an optical cavity(Maunz *et al.* (2004); McKeever *et al.* (2003); Nußmann *et al.* (2005)). The explanation of the cooling process, where cooling rate is positively measured by the number of atoms in the system, is one of the outstanding properties of many system cooling (Domokos & Ritsch (2002)).

However it remains challenging to theoretically describe the cooling process cavity-mediated for many body systems[1]. There have been a number of semiclassical approaches to give a qualitative description, but even complete quantum mechanical models find it difficult to explain the collective nature of cavity-mediated laser cooling and the extremely low phonon numbers it provides.

1.3 Quantum sonoluminescence

Sonoluminescence can be defined as a phenomenon of strong light emission from gas bubble collapses which contains many atoms which are acoustically confined and periodically driven in a liquid by ultrasonic frequencies. For example, during the collapse phase of a typical single-bubble sonoluminescence experiment, the

[1]The terms “atoms” and ”ions” are both used in the thesis interchangeably, since the charge of the atomic particles does not matter for the cooling process.

bubble is considered to be thermally isolated from their surrounding particles. The collapse phase is followed by the immediate emission of light which indicates very high temperature inside the bubble. At the beginning of the following expansion phase, the bubble oscillates about its equilibrium radius until it returns to its stability. This process indeed regenerates itself with unusual precision. From a quantum optics perspective, there are many similarities between ion trap and sonoluminescence experiments (Gaitan *et al.* (1992); Lohse (2002)).

Though extensively investigated sonoluminescence, the origin of the energy concentration remains a mystery during the final phase of the bubble collapse (Putterman *et al.* (2001); Suslick & Flannigan (2008)). A valid theoretical model can include a plasma formation mechanism and a mechanism that can further increase the plasma temperature by at least one order of magnitude. It must be possible for the mechanism to operate in a strong, state-like environment and on a very small bubble radius length scale.

In order to measure the spectrum from the picosecond light flash at the end of the collapse and associate the continuum behind the black-body or Bremsstrahlung spectra, at least the temperature in the bubble indicates that the temperature of at least the same is $10^3 - 10^4\,K$ (Barber & Putterman (1991); Didenko *et al.* (2000); Suslick & Flannigan (2008)). Light emissions in the ultraviolet regime can also be seen which indicate temperatures approximately $10^6\,K$, as Camara *et al.* (2004) showed. It is noteworthy that the highly excited energy populations are identified with noble gas and metal atoms, which are not thermally populated, but which show the presence of a dense plasma. It should also be noted that sharp lines of emission are found within an optical system (Brenner *et al.* (2002); Flannigan & Suslick (2007); Suslick & Flannigan (2008)).

1.4 Structure of the thesis

Although the idea of laser cooling and also cavity mediated laser cooling are not new ones, this thesis seeks to develop a new formalism which provides further insights into the complex dynamics present when particle and cavity field interact. In this thesis, we design a cooling scheme and provide a complete quantum-mechanical description. The plan of this thesis is to discuss aspects

related to the similarities between quantum optics experiments with trapped ions and cavitating bubbles. These suggest that both could be cooled to extremely low temperatures. Cooling atoms in cavitating bubbles may have applications in micro- and nanotechnology, which require very small volume cooling. We examine the physical processes underlying the recently proposed quantum heat exchanger and provide additional guidance for quantum optics experiments with cavitating bubbles. Here, we assume that the bubbles will always remain transparent and estimate the cooling rates that can be achieved. It is demonstrated that a cooling laser can transfer a single collective phonon mode to extremely low temperatures during the bubble collapse phase. Additionally, we see that the atomic dynamics between collapse phases results in an efficient redistribution of thermal energy. This thesis contains two main parts: the first one consists of the background of the laser cooling techniques and the second part of the thesis is original new material. The details are as follows below:

Part 1, the first part mainly contains a specific review of concepts involved and consists of three chapters. The purpose of Chapter 2 is to introduce an overview of the features of laser cooling techniques. As we shall see later, these techniques can be implemented more easily and are expected to be much more efficient for many atoms in cavitating bubbles. Chapter 3 outlines the theory of quantum harmonic oscillators. Afterwards, Chapter 4 introduces an overview of the sonoluminescence phenomenon and provides a more detailed idea of this phenomenon.

Part 2 focuses on the intriguing phenomenon of sonoluminescence. In this Part, different approaches will be discussed that introduce master equations describing the system effectively on a coarse grained time scale. A toy-model is proposed in order to explain the origin of the sudden energy concentration in this phenomenon. The model is built on theories used in order to explain laser cooling experiments and understands the sonoluminescence as an open quantum system of strongly confined particles. The purpose of Chapter 5 is to provide an introduction to the design of a quantum heat exchanger for nanotechnology which converts heat into light on relatively short quantum optical time scales. This scheme takes advantage of both heat transfer and collective cavity-mediated laser cooling of an atomic gas inside a cavitating bubble. In Chapter 6 laser

cooling of indistinguishable particles in cavitating bubbles is examined analytically. Chapter 7 will conclude with a discussion and possible quantum optical enhancement schemes. Furthermore, it will outline some ideas for future work.

Part 1: Background

Chapter 2

Overview of laser cooling techniques

This chapter introduces some background material on laser cooling. As we shall see below, we first describe the principle of laser cooling. Afterwards, we introduce a brief history of laser cooling as well as laser cooling of individually trapped particles.

2.1 Laser cooling atoms

In the second half of the 20^{th} century, laser cooling in ions played a major role in the development of physics. It is an interesting opportunity to explore quantum phenomena and provide a testing ground for theory to slow ions down and spatially confine them with almost resonant light. Laser cooling is thus a major factor in metrology, improving the accuracy of atomic clocks dramatically. The first scalable quantum computing architecture that complies with many of the DiVinzenco criteria was the Laser Cooling (DiVincenzo (1995)), which also enabled us to achieve the quantum degeneracy system (Cornell & Wieman (2002)).

2.1.1 The principle of laser cooling

Resonant laser light is an efficient way to manage the motion of an atom. The principle behind is very straightforward. When an atom of the mass m absorbs

a photon from an atomically transiently resonant light field, a momentum kick is given to the laser beam (or the $\vec{k}$ - vector of light) in the direction of the propagation. Upon absorption, the velocity of the atom decreases by the speed of recoil $v_r = \hbar k/m$. Before it again absorbs a photon, the atom must decay from its excited state. However, a spontaneous emission, which has no net impact on atomic motion is a spatially isotropic process. The atom is slowed preferably in the direction of laser propagation after many spontaneous cycles of absorption. The power the laser field exerts on atomic motion is the spontaneous or dispersing power we will consider. In general, the laser frequency is slightly under the atomic frequency of transition. Then, in order for the atom to absorb a photon, it must move at a speed v to the laser beam that shifts it to the laser light resonance. This results in a net force which is proportional to its velocity and is called 'Doppler cooling' against the atomic motion. This viscous force can be used to capture the ions into a so-called 'optical molasses' across all spatial dimensions.

2.1.2 A brief history of laser cooling

The interaction between atoms and light has been theoretically and experimentally studied for a long time. Hänsch & Schawlow (1975) made the first attempts to describe laser cooling, and Wineland & Dehmelt (1975) did so independently for trapped ions. It was discovered that the scattering of light from single particles affected the particles' external motion. Such effects resulted in significant changes in the vibrational energy of massive particles. Several other laser cooling techniques have been developed, allowing atoms and ions to be cooled to the micro and nanokelvin temperatures required for quantum coherence and degeneracy (Chu (1998); Cohen-Tannoudji (1998); Phillips (1998)). Sisyphus cooling (Cohen-Tannoudji & Phillips (1990)) and evaporative cooling (Ketterle & Van Druten (1996)) are two examples of these.

It is not surprising that laser cooling was shown first as it is located in space with trapped ions. The first experiments to show the effect of laser cooling in neutral atoms sought to slow the atomic beam with the laser light, which contradicts the atomic motion.

2.1.3 Laser cooling of individually trapped particles

For laser cooling to be at its most efficient, the confinement of individually trapped particles should be so strong that the quantum characteristics of their motion is no longer negligible. This means, their vibrational energy is made up of energy quanta which have been named phonons. When this applies, an externally applied laser field not only affects the electronic states of a trapped ion—it also changes its vibrational state. Ideally, laser frequencies should be chosen such that the excitation of the ion should be most likely accompanied by the loss of a phonon. If the ion returns subsequently into its ground state via the spontaneous emission of a photon, its phonon state remains the same. Overall one phonon is permanently lost from the system which implies cooling. On average, every emitted photon lowers the vibrational energy of the trapped ion by the energy of one phonon. Eventually, the cooling process stops when the ion no longer possesses any vibrational energy. This state was no vibration and energy which corresponds to the stationary state of the system.

Currently, there are many different ways of designing and fabricating ion traps (Goodwin *et al.* (2016); Stick *et al.* (2006)). However, the main requirements for the efficient conversion of vibrational energy into light on relatively short quantum optical time scales are always the same (Blake *et al.* (2011b); Stenholm (1986)):

1) Individual atomic particles need to be so strongly confined that the quantum character of their motion has to be taken into account. In the following, ν denotes the phonon frequency and $\hbar\nu$ is the energy of a single phonon. The thesis regularly refers to "frequencies" which are strictly angular frequencies, as usually done in quantum optics.

2) A laser field with a frequency ω_{L} below the atomic transition frequency ω_0 needs to be applied. As long as the laser detuning $\Delta = \omega_0 - \omega_{\mathrm{L}}$ and the phonon frequency ν are comparable in size,

$$\Delta \sim \nu\,, \tag{2.1}$$

the excitation of an ion is more likely accompanied by the annihilation of a phonon than by the creation of a phonon. Transitions which result in the

simultaneous excitation of an ion and the creation of a phonon are possible but are less likely to occur as long as their detuning is larger.

3) When excited, the confined atomic particle needs to be able to emit a photon. In the following, we denote its spontaneous decay rate by Γ. This rate should not be much larger than ν,

$$\nu \;\geq\; \Gamma\,, \tag{2.2}$$

so that the cooling laser couples efficiently to atomic transitions. At the same time, Γ should not be too small so that de-excitation of the excited atomic state happens often via the spontaneous emission of a photon.

Given these three conditions, the applied laser field results in the conversion of the vibrational energy of individually trapped ions into photons. As mentioned already above, laser cooling can prepare individually trapped atomic particles at low enough temperatures for applications in high-precision quantum optics experiments and in quantum technology.

Fig. 2.1(a) shows a single two-level atom (or ion) with external laser driving inside an approximately harmonic trapping potential. Most importantly, the atom should be so strongly confined that its phonon states are no longer negligible. In the following, ν denotes the frequency of the energy quanta in the vibrational energy of the atomic particle and $|m\rangle$ is a vibrational state with exactly m phonons. Moreover, $|\mathrm{g}\rangle$ and $|\mathrm{e}\rangle$ denote the ground and the excited electronic state of the trapped particle with energy separation $\hbar\omega_0$. Fig. 2.1(b) shows the energy level of the combined atom-phonon system with the energy eigenstates $|\mathrm{x}, m\rangle$.

To lower the temperature of the atom, the frequency ω_L of the cooling laser needs to be below its transition frequency ω_0. Ideally the laser detuning $\Delta = \omega_0 - \omega_\mathrm{L}$ equals the phonon frequency ν (cf. Eq. (2.1)). In addition, the spontaneous decay rate Γ of the excited atomic state should not exceed ν (cf. Eq. (2.2)). When both conditions apply, the cooling laser couples most strongly, i.e. resonantly and efficiently, to transitions for which the excitation of the atom is accompanied by the simultaneous annihilation of a phonon. All other transitions are strongly detuned. Moreover, the spontaneous emission of a photon only affects the electronic but not the vibrational states of the atom. Hence, the spontaneous

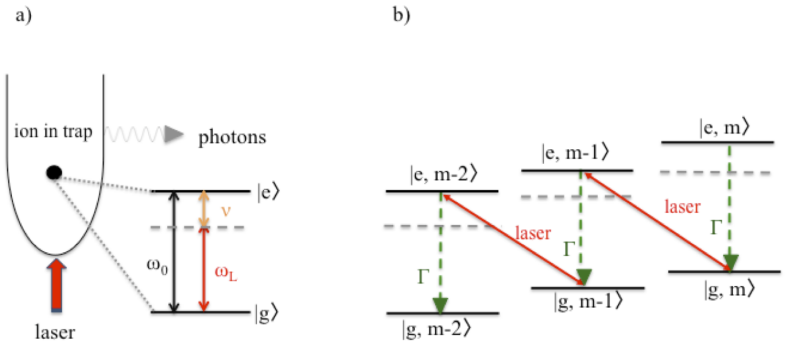

Figure 2.1: (a) Schematic view of the experimental setup for laser cooling of a single trapped ion. Here $|\mathrm{g}\rangle$ and $|\mathrm{e}\rangle$ denote the ground and the excited state of the ion, respectively, with transition frequency ω_0 and spontaneous decay rate Γ. The motion of the particle is strongly confined by an external harmonic trapping potential such that its quantum nature can no longer be neglected. Here, ν denotes the frequency of the corresponding phonon mode and ω_L is the frequency of the applied cooling laser. (b) The purpose of the laser is to excite the ion, while annihilating a phonon, thereby causing transitions between the basis states $|\mathrm{x}, m\rangle$ with $\mathrm{x} = \mathrm{g}, \mathrm{e}$ and $m = 0, 1, \ldots$ of the atom-phonon system. If the excitation of the ion is followed by the spontaneous emission of a photon, a phonon is permanently lost which implies cooling.

emission of a photon usually indicates the loss of one phonon. Suppose the atom was initially prepared in a state $|\mathrm{g}, m\rangle$. Then its final state equals $|\mathrm{g}, m-1\rangle$. One phonon has been permanently removed from the system which implies cooling. As illustrated in Fig. 2.1(b), the trapped particle eventually reaches its ground state $|\mathrm{g}, 0\rangle$ where it no longer experiences the cooling due to off-resonant driving (Blake *et al.* (2011b); Stenholm (1986)).

To a very good approximation, the Hamiltonian of the atom-phonon system equals Blake *et al.* (2011b)

$$H_\mathrm{I} \;=\; \hbar g \left(\sigma^- b^\dagger + \sigma^+ b\right) \tag{2.3}$$

in the interaction picture with respect to its free energy. Here g denotes the (real) atom-phonon coupling constant, while $\sigma^+ = |\mathrm{e}\rangle\langle\mathrm{g}|$ and $\sigma^- = |\mathrm{g}\rangle\langle\mathrm{e}|$ are atomic raising and lowering operators. Moreover, b and $b^\dagger$ are phonon annihilation and

creation operators with $[b, b^\dagger] = 1$. To take into account the spontaneous emission of photons from the excited state of the atom with decay rate Γ, we describe the atom-phonon system in the following by its density matrix $\rho_{\rm I}(t)$ with

$$\dot{\rho}_{\rm I} = -\frac{i}{\hbar}[H_{\rm I}, \rho_{\rm I}] + \Gamma\left(\sigma^- \rho_{\rm I} \sigma^+ - \frac{1}{2}\sigma^+\sigma^- \rho_{\rm I} - \frac{1}{2}\rho_{\rm I}\sigma^+\sigma^-\right). \tag{2.4}$$

This equation can be used to analyse the dynamics of the expectation value $\langle A_{\rm I}\rangle = {\rm Tr}(A_{\rm I}\rho_{\rm I})$ of observables $A_{\rm I}$, since it implies

$$\langle \dot{A}_{\rm I}\rangle = -\frac{\rm i}{\hbar}[A_{\rm I}, H_{\rm I}] + \Gamma\left\langle \sigma^+ A_{\rm I} \sigma^- - \frac{1}{2}A_{\rm I}\sigma^+\sigma^- - \frac{1}{2}\sigma^+\sigma^- A_{\rm I}\right\rangle. \tag{2.5}$$

Here we are especially interested in the dynamics of the mean phonon number $m = \langle b^\dagger b\rangle$. In order to obtain a closed set of rate equations, we also need to study the dynamics of the population of the excited atomic state $s = \langle\sigma^+\sigma^-\rangle$ and the dynamics of the atom-phonon coherence $k_1 = {\rm i}\,\langle\sigma^- b^\dagger - \sigma^+ b\rangle$. Using Eq. (2.5), one can show that

$$\begin{aligned} \dot{m} &= -g\,k_1\,, \\ \dot{s} &= g\,k_1 - \Gamma\,s\,, \\ \dot{k}_1 &= 2g(m-s) - 4g\,ms - \frac{1}{2}\Gamma\,k_1 \end{aligned} \tag{2.6}$$

when assuming that $\langle\sigma^+\sigma^- b^\dagger b\rangle = \langle\sigma^+\sigma^-\rangle\langle b^\dagger b\rangle = ms$ to a very good approximation. Having a closer look at the above equations, we see that the system rapidly reaches its stationary state with $m = s = k_1 = 0$. Eventually, the atom reaches a very low temperature. More detailed calculations reveal that the final phonon number m of the trapped atom depends on its system parameters but remains small as long as the ratio Γ/ν is sufficiently small Blake *et al.* (2011b). The above cooling equations (2.6) also show that the corresponding cooling rate equals

$$\gamma_{\rm 1\,atom}^{\rm standard} = g^2/\Gamma \tag{2.7}$$

to a very good approximation and that the cooling process takes place not on mechanical but on relatively short quantum optical time scales.

2.2 Cavity-mediated laser cooling

In this section, we first describe the principle of cavity-mediated laser cooling. Afterwards, we introduce a brief history of cavity-mediated laser cooling, cavity-mediated laser cooling of a single atom as well as cavity-mediated collective laser cooling.

2.2.1 The principle of cavity-mediated laser cooling

For laser cooling of a single atom, two major regimes are distinguished. For example, the final temperature is limited to $T = \frac{\hbar\Gamma}{2k_B}$ in the limit of the weak coupling, if the frequency ν of the trap is below the natural line width Γ of the optical transition of the atom. The Doppler cooling limit is commonly referred to as a dazzle. However, when the trap frequency is higher than its natural line width, as it is in the strong-binding limit and the atom develops well-resolved sidebands of absorption. The cooling laser can therefore be tuned to one of the sidebands and the atom can be cooled to its lowest vibration level. The whole thing is known as sideband cooling. The cooling limitations in both Doppler and sideband cooling were found experimentally and in good agreement with the theory (Diedrich *et al.* (1989)).

During a lot of Quantum Optics experiments, laser sideband cooling was a prime method, because of its ability to cool a single atom to very low temperatures. It also has certain drawbacks, such as not being able simultaneously to cool large numbers of atoms efficiently or to cool particles with complex level structures, such as molecules (Lev *et al.* (2008)), as mentioned earlier. Proposals were made for alternative techniques. One suggestion is that the sideband regime works while the atomic system is confined to an optical cavity. Thereto the interaction between the system and the radiation field surrounding it strongly enhances. Furthermore, cavity cooling does not depend on spontaneous atomic emissions, and cavity geometries can be manipulated. However, as we shall see below, laser cooling of many atoms results only in the cooling of one collective mode.

2.2.2 A brief history of cavity-mediated laser cooling

In Vigneron (1995), initial indications of cavity-mediated laser cooling were found for atomic systems. McKeever *et al.* (2003) reported the successful cooling and trapping of individual cesium atoms. In Maunz *et al.* (2004) cooling mechanisms have been shown to lead to extended storage times and better location of the atoms. In comparison with that observed in free air cooling, the cooling rate has been estimated to be at least five times higher. Nußmann *et al.* (2005) showed that the orthogonal laser cooling, laser and cavity-axis configuration lead to high cooling efficiency, low temperatures and relatively long trapping times. Wolke *et al.* (2012) stated an atom-cavity system with a cavity bandwidth below the recoil limit and cooling at densities and temperatures incompatible with conventional laser cooling. A single atom cooling system in an optical cavity with electromagnetically induced transparency was observed with the two-photon resonance at Kampschulte *et al.* (2010). In Chuah *et al.* (2013) the cavity cooling of a single ion was investigated beyond the Lamb-Dicke system, showing a cooling threshold below the Doppler temperature.

Mossberg *et al.* (1991) and Zaugg *et al.* (1993) stated that the use of an optical resonator can greatly enhance atomic cooling. Domokos & Ritsch (2003) later identified weak and strong coupling regimes, using the half-classical approach and emphasized the importance of particle correlations. Hemmerling & Robb (2011) demonstrated cooling using a blue-detuned driving light. Furthermore, the number of atoms has enhanced the cooling rate within the configuration of the atom pump while the cavity pump configuration is without effect. The addition of cavity, as shown by Murr (2006), leads in the Doppler limit to change the Doppler force. Vuletić & Chu (2000) has proposed a laser cooling method for low saturation atoms and high detuning.

Although the semiclassical approach can describe a number of phenomena of laser cooling through cavity-mediated, Cirac *et al.* (1993) master equation approach provides for a complete quantum mechanical description of the cooling process. The cooling of the cavity at very low temperatures where the quantum effects prevails over the system and semiclassical models can no longer be used (

Domokos & Ritsch (2003)). This is particularly useful in cavity cooling. Moreover, master equation calculations are more precisely controlled than semiclassical calculations. Afterwards, many authors used a master equation approach. Cirac *et al.* (1995) have dealt with bad cavity and low saturation levels, showing that even in strong containment conditions, an atom can be cooled in the trap ground state.

Beige *et al.* (2005), in which the particles are coupled with the quantum field of an optical cavities and driven by a red-detuned laser field, proposed a mechanism for collective cooling for a large number of trapped particles. In Blake *et al.* (2011a, 2012), the cavity-mediated laser cooling was compared to normal sideband laser cooling. It showed that both the techniques exhibit striking similarities within the range of validity of the Lamb-Dicke approximation. For instance, in weak and strong containment regimes the mean number of phonon stationary states are expressed in the same way. The cooling of many-body systems in an optical cavity is much richer and more complicated compared to individual particles. Later, it will be identified or understood much less than that. There have been reports of multiple systematic experimental studies. Schleier-Smith *et al.* (2011) showed the cooling, down to two phonons in a good agreement with an Optomechanical Model, of the single collective vibrational mode of an atomic ensemble. The rate of cooling was proportional to the ensemble's total photon spread rate which showed the light-inducing cooling method collectively.

2.2.3 Cavity-mediated laser cooling of a single atom

Suppose we want to cool a single atom whose transition frequency ω_0 is well above the optical regime, i.e. much larger than typical laser frequencies ω_L. In this case, it is impossible to realise the condition $\Delta \sim \nu$ in Eq. (2.1). Hence it might seem impossible to lower the temperature of the atom via laser cooling. To overcome this problem, we confine the particle in the following inside an optical resonator (cf. Fig. 2.2) and denote the cavity state with exactly n photons by $|n\rangle$. Using this notation, the energy eigenstates of the atom-phonon-photon systems can be written as $|\mathrm{x}, m, n\rangle$. Moreover, ν is again the phonon frequency, κ denotes the

spontaneous cavity decay rate and ω_{L} and ω_{cav} denote the laser and the cavity frequency, respectively.

In the experimental setup in Fig. 2.2, all transitions which result in the excitation of the atom are naturally strongly detuned and can be neglected. However, the same does not have to apply to indirect couplings which result in the direct conversion of phonons into cavity photons (Blake *et al.* (2011a); Kim *et al.* (2018)). Suppose the cavity detuning $\Delta_{\mathrm{cav}} = \omega_{\mathrm{cav}} - \omega_{\mathrm{L}}$ and the phonon frequency ν are approximately the same and the cavity decay rate κ does not exceed ν,

$$\Delta_{\mathrm{cav}} \sim \nu \quad \text{and} \quad \nu \geq \kappa\,, \tag{2.8}$$

in analogy to Eqs. (2.1) and (2.2). Then two-step transitions which excite the atom while annihilating a phonon immediately followed by the de-excitation of the atom while creating a cavity photon become resonant and dominate the dynamics of the atom-phonon-photon system. The overall effect of these two-step transitions is the direct conversion of a phonon into a cavity photon, while the atom remains essentially in its ground state (cf. Fig. 2.2(b)). When a cavity photon subsequently leaks into the environment, the phonon is permanently lost.

To model the above described dynamics, we describe the experimental setup in Fig. 2.2 in the following by the interaction Hamiltonian (Blake *et al.* (2011a); Kim & Beige (2013))

$$H_{\mathrm{I}} \;=\; \hbar g_{\mathrm{eff}} \left(b c^{\dagger} + b^{\dagger} c \right), \tag{2.9}$$

where g_{eff} denotes the effective atom-cavity coupling constant and where c with $[c, c^{\dagger}] = 1$ is the cavity photon annihilation operator. Since the atom remains essentially in its ground state, its spontaneous photon emission remains negligible. To model the possible leakage photons through the cavity mirrors, we employ again a master equation. Doing so, the time derivative of the density matrix $\rho_{\mathrm{I}}(t)$ of the phonon-photon system equals

$$\dot{\rho}_{\mathrm{I}} \;=\; -\frac{\mathrm{i}}{\hbar}[H_{\mathrm{I}}, \rho_{\mathrm{I}}] + \kappa \left(c \rho_{\mathrm{I}} c^{\dagger} - \frac{1}{2} c^{\dagger} c \rho_{\mathrm{I}} - \frac{1}{2} \rho_{\mathrm{I}} c^{\dagger} c \right) \tag{2.10}$$

in the interaction picture. Hence, expectation values $\langle A_{\mathrm{I}} \rangle = \mathrm{Tr}(A_{\mathrm{I}} \rho_{\mathrm{I}})$ of phonon-photon observables A_{I} evolve such that

$$\langle \dot{A}_{\mathrm{I}} \rangle \;=\; -\frac{\mathrm{i}}{\hbar}[A_{\mathrm{I}}, H_{\mathrm{I}}] + \kappa \left\langle c^{\dagger}\, A_{\mathrm{I}}\, c - \frac{1}{2} A_{\mathrm{I}}\, c^{\dagger} c - \frac{1}{2} c^{\dagger} c\, A_{\mathrm{I}} \right\rangle , \tag{2.11}$$

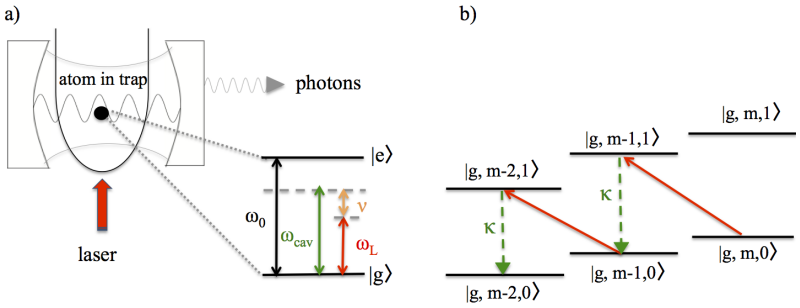

Figure 2.2: (a) Schematic view of the experimental setup for cavity-mediated laser cooling of a single atom. The main difference between this setup and the setup shown in Fig. 2.1 is that the atom now couples in addition to an optical cavity with frequency $\omega_{\rm cav}$ and the spontaneous decay rate κ. Here both the cavity field and the laser are highly detuned from the atomic transition and the direct excitation of the atom remains negligible. However the cavity detuning $\Delta_{\rm cav} = \omega_{\rm cav} - \omega_{\rm L}$ should equal the phonon frequency of the trapped particle. (b) As a result, only the annihilation of a phonon accompanied by the simultaneous creation of a cavity photon are in resonance. In cavity-mediated laser cooling, the purpose of the laser is to convert phonons into cavity photons. The subsequent loss of this photon via spontaneous emission results in the permanent loss of a phonon and therefore in the cooling of the trapped particle.

in analogy to Eq. (2.5). In the following, we use this equation to study the dynamics of the phonon number $m = \langle b^\dagger b\rangle$, the photon number $n = \langle c^\dagger c\rangle$ and the phonon-photon coherence $k_1 = {\rm i}\langle bc^\dagger - b^\dagger c\rangle$. Proceeding as described in the previous subsection, we now obtain the rate equations

$$\begin{aligned} \dot m &= g_{\rm eff} k_1 \,, \\ \dot n &= -g_{\rm eff} k_1 - \kappa n \,, \\ \dot k_1 &= 2g_{\rm eff}(n-m) - \frac{1}{2}\kappa k_1 \,. \end{aligned} \tag{2.12}$$

These describe the continuous conversion of phonons into cavity photons which subsequently escape the system. Hence it is not surprising to find that the stationary state of the atom-phonon-photon system corresponds to $m = n = k_1 = 0$. Independent of its initial state, the atom again reaches a very low temperature.

In analogy to Eq. (2.7), the effective cooling rate for cavity-mediated laser cooling is now given by Blake *et al.* (2011a); Kim & Beige (2013)

$$\gamma_{1\,\mathrm{atom}} \;=\; g_{\mathrm{eff}}^2/\kappa\,. \tag{2.13}$$

Due to the resonant coupling being indirect, g_{eff} is in general a few orders of magnitude smaller than g in Eq. (2.7), if the spontaneous decay rates κ and Γ are of similar size. Cooling a single atom inside an optical resonator might therefore take significantly longer. However, as we shall see below, this reduction in cooling rate can be compensated for by the collective enhancement of the atom-cavity interaction constant g_{eff} (Beige *et al.* (2005)).

2.2.4 Cavity-mediated collective laser cooling

In previous subsections, we had a closer look at a standard laser cooling technique for an individually trapped atomic particle (Blake *et al.* (2011b); Stenholm (1986)). We also reviewed cavity-mediated laser cooling of a single atom (Blake *et al.* (2011a); Cirac *et al.* (1993, 1995); Kim & Beige (2013); Uruñuela *et al.* (2020)) and of an atomic gas (Beige *et al.* (2005); Kim *et al.* (2018)). Next we introduce cavity-mediated collective laser cooling of an atomic gas inside an optical resonator (Beige *et al.* (2005); Kim *et al.* (2018)). To do so, we replace the single atom in the experimental setup in Fig. 2.2 by a collection of N atoms. In analogy to Eq. (2.9), the interaction Hamiltonian H_{I} between phonons and cavity photons now equals

$$H_{\mathrm{I}} \;=\; \sum_{i=1}^{N} \hbar g_{\mathrm{eff}}^{(i)} \left(b_i c^\dagger + b_i^\dagger c \right)\,, \tag{2.14}$$

where $g_{\mathrm{eff}}^{(i)}$ denotes the effective atom-cavity coupling constant of atom i. This coupling constant is essentially the same as g_{eff} in Eq. (2.13) and depends in general on the position of atom i. Moreover b_i denotes the phonon annihilation operator of atom i with $[b_i, b_j^\dagger] = \delta_{ij}$. In order to simplify the above Hamiltonian, we introduce a collective phonon annihilation operator B,

$$B = \frac{\sum_{i=1}^{N} g_{\mathrm{eff}}^{(i)}\, b_i}{\tilde{g}_{\mathrm{eff}}} \qquad \text{with} \qquad \tilde{g}_{\mathrm{eff}} = \left(\sum_{i=1}^{N} |g_{\mathrm{eff}}^{(i)}|^2 \right)^{1/2}\,, \tag{2.15}$$

with $[B, B^\dagger] = 1$. Using this notation, H_I in Eq. (2.14) simplifies to

$$H_\mathrm{I} \;=\; \hbar\tilde{g}_\mathrm{eff}\left(Bc^\dagger + B^\dagger c\right) . \tag{2.16}$$

Notice that the effective coupling constant $\tilde{g}_\mathrm{eff}$ scales as the square root of the number of atoms N inside the cavity. For example, if all atomic particles couple equally to the cavity field with a coupling constant $g_\mathrm{eff} \equiv g_\mathrm{eff}^{(i)}$, then $\tilde{g}_\mathrm{eff} = \sqrt{N}\, g_\mathrm{eff}$. This means, in case of many atoms, the effective phonon-photon coupling is collectively enhanced (Beige *et al.* (2005)).

When comparing H_I in Eq. (2.9) with H_I in Eq. (2.14), we see that both Hamiltonians are essentially the same. Moreover the density matrix ρ_I obeys the master equation in Eq. (2.10) in both cases. Hence we expect the same cooling dynamics in the one atom and in the many atom case. Suppose all atoms experience the same atom-cavity coupling constant g_eff, the effective cooling rate of the common vibrational mode B becomes

$$\gamma_{N\,\mathrm{atoms}} \;=\; N g_\mathrm{eff}^2/\kappa\,, \tag{2.17}$$

in analogy to Eq. (2.13). This cooling rate is N times larger than the cooling rate which we predicted in the previous subsection for cavity-mediated laser cooling of a single atom. Using sufficiently large number of atoms N, it is therefore possible to realise cooling rates $\gamma_{N\,\mathrm{atoms}}$ with

$$\gamma_{N\,\mathrm{atoms}} \;\gg\; \gamma_{1\,\mathrm{atom}}^{\mathrm{standard}} . \tag{2.18}$$

This suggests that the cooling rate of cavity-mediated laser cooling, i.e. the rate of change of the mean number n of B phonons in the system, is comparable and might even exceed the cooling rates of standard laser cooling of single trapped ions.

However, the above discussion also shows that cavity-mediated collective laser cooling only removes phonons from a single common vibrational mode B, while all other vibrational modes of the atomic gas do not experience the cooling laser. Once the B mode reaches its stationary state, the conversion of thermal energy into light stops. To nevertheless take advantage of the relatively high cooling rates of cavity-mediated collective laser cooling, an additional mechanism is needed

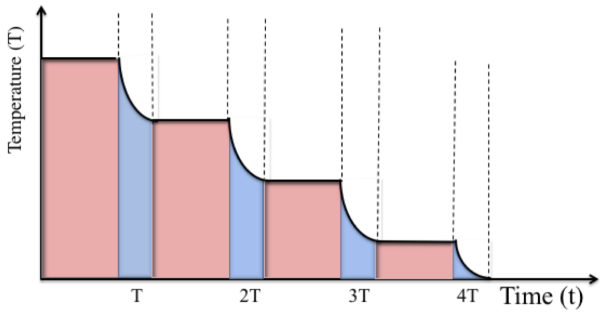

Figure 2.3: Schematic view of the expected dynamics of the temperature of the atomic gas during cavity-mediated collective laser cooling which involves a sequence of cooling stages (blue) and thermalisation stages (pink). During thermalisation stages, heat is transferred from the different vibrational degrees of freedoms of the atoms into a certain collective vibrational mode B, while the mean temperature of the atoms remains the same. During cooling stages, energy transfer from the B mode into light. Eventually, the atomic gas becomes very cold.

(Kim *et al.* (2018)). As we shall see in the next section, one way of transferring energy between different vibrational modes is to intersperse cooling stages with thermalisation stages (cf. Fig. 2.3). The purpose of the cooling stages is to rapidly remove energy from the system. The purpose of subsequent thermalisation stages is to transfer energy from the surroundings of the bubble and from the different vibrational modes of the atoms into the B mode. Repeating thermalisation and cooling stages is expected to result in the cooling of the whole setup.

2.3 Summary

This chapter has focused our attention on the material on laser cooling techniques. As we shall see above, we described the principle of laser cooling. In addition, we introduced a brief history of laser cooling as well as laser cooling of individually trapped particles. In section 2.2, we reviewed cavity-mediated laser cooling of a single atom (Blake *et al.* (2011a); Cirac *et al.* (1993, 1995); Kim & Beige (2013); Uruñuela *et al.* (2020)) and of an atomic gas (Beige *et al.* (2005); Kim *et al.*

(2018)). We introduced cavity-mediated collective laser cooling of an atomic gas inside an optical resonator (Beige *et al.* (2005); Kim *et al.* (2018)).

Chapter 3

Quantum harmonic oscillators

3.1 Introduction

The quantum harmonic oscillator is one of the most basic and essential systems in quantum mechanics. The theory used to solve a simple quantum harmonic oscillator is crucial to understanding quantum mechanics. In this thesis, we focus on cooling trapped particles that are confined to a harmonic potential. In this environment, a full quantum description may be made of the cooling process, as the cooling process can transfer the initial vibrational state of the particle to the motional ground state. In this Chapter, we introduce the formalism that we will use in the rest of the thesis: the theory of the quantum harmonic oscillators. More detailed knowledge of the content can be found in the literature (Gerry *et al.* (2005); Haroche & Raimond (2006)).

Section 3.2 develops the basis of the quantum approach to harmonic oscillators. The dimensionless creation and annihilation operators are first introduced. We start with the quantisation of a harmonic oscillator and present the description of its eigenstates, so-called number states, and energy levels in the quantisation. Number states will be used to characterise the vibrational states of the trapped particles and cavity radiation modes in the chapters that follow.

Section 3.3 is concerned with the theory for harmonic oscillators in the thermal state. As the thermal state of a harmonic oscillator is indeed a mixed state, a canonical density operator can describe it. We use the density operator to

calculate the thermal average of the number operator and link it to the vibrational energy of the system (Blais *et al.* (2020)).

3.2 Quantisation of harmonic oscillator

A knowledge of the quantized level of energy initially introduced by Planck (1901) is the most important finding concerning the quantum harmonic oscillators to explain the spectral density of a black body through

$$E_m = m\,\hbar\nu \qquad \text{with} \qquad m = 1, 2, \ldots . \tag{3.1}$$

This assumed the expression in Heisenberg's matrix mechanics of the quantized energy levels later, and this showed that they were given by

$$E_m = \left(m + \frac{1}{2}\right)\hbar\nu \qquad \text{with} \qquad m = 0, 1, 2, \ldots . \tag{3.2}$$

From a quantum mechanics perspective, the problem is to solve the eigenvalue equation of the Hamiltonian. One option is to solve the second-order partial differential equation, i.e. a time-independent Schrödinger equation, the wave mechanics picture of the equation. This approach requires some understanding of the theory of partial differential equations. The other option is to deduce two new operators, the ladder operators, from the position and momentum of Hermitian operators, which enable the eigenvalue equation of the Hamiltonian to be readjusted easily.

Remember that the following Hamiltonian can describe a single one-dimensional mass M oscillator in a harmonic trap with frequency ν that is (Loudon (2000))

$$H \;=\; \frac{p^2}{2M} + \frac{1}{2}\,M\nu^2 x^2\,, \tag{3.3}$$

Where its momentum operator p and position operator x have the usual commutator relationship,

$$[x, p] \;=\; i\hbar\,. \tag{3.4}$$

When it is not important for the exact shape of the wave function of the harmonic oscillator, the second quantisation and the ladder operators are introduced,

$$\begin{aligned} b &= \sqrt{\frac{M\nu}{2\hbar}} + \left(x + \frac{\mathrm{i}}{M\nu} p \right) , \\ b^\dagger &= \sqrt{\frac{M\nu}{2\hbar}} + \left(x - \frac{\mathrm{i}}{M\nu} p \right) . \end{aligned} \tag{3.5}$$

This refers to the b and $b^\dagger$ of the operators following the commutator relationship,

$$[b, b^\dagger] = 1 . \tag{3.6}$$

Applying Eqs. (3.5), the Hamiltonian (3.3) is converted to

$$H = \hbar\nu \left(b^\dagger b + \frac{1}{2} \right) . \tag{3.7}$$

To help address the Schrödinger equation, consider an arbitrary eigenstate $|m\rangle$ with relative eigenvalue E_m. The Schrödinger equation then can be written as

$$H|m\rangle = \hbar\nu \left(b^\dagger b + \frac{1}{2} \right) |m\rangle = E_m |m\rangle . \tag{3.8}$$

Multiplying both sides from the left by $b^\dagger$ gives

$$\hbar\nu \left(b^\dagger \, b^\dagger b + \frac{1}{2} b^\dagger \right) |m\rangle = E_m b^\dagger |m\rangle \tag{3.9}$$

$$\hbar\nu \left(b^\dagger \, b b^\dagger - \frac{1}{2} b^\dagger \right) |m\rangle = E_m b^\dagger |m\rangle \tag{3.10}$$

$$\hbar\nu \left(b^\dagger b + \frac{1}{2} \right) b^\dagger |m\rangle = (E_m + \hbar\nu) b^\dagger |m\rangle . \tag{3.11}$$

The last equation represents an expression of an energy eigenvalue equation with the eigenstate

$$|m+1\rangle = b^\dagger |m\rangle \tag{3.12}$$

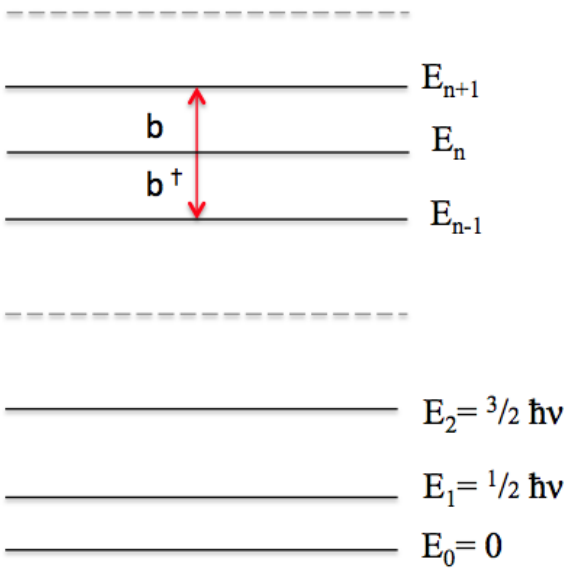

Figure 3.1: Configuration of energy levels for the quantum-mechanical harmonic oscillator. In the case of the operators of creation $b^\dagger$ and the operators of destruction b, an amount $\hbar\nu$ will be respectively added or subtracted.

and the eigenvalue $E_{m+1} = E_m + \hbar\nu$. As it can be seen, there exists another level greater than the first by the amount $\hbar\nu$. The energy level consists of a ladder with equal spacing without a top limit, as shown in Fig. 3.1. The use of the so-called creation operator $b^\dagger$ to transfer the energy to an increasing level. In the same way, the use of the destruction operator b shifts the energy level downwards,

$$H\, b|m\rangle \;=\; (E_m - \hbar\nu) b|m\rangle\,, \tag{3.13}$$

with respect to the state

$$|m-1\rangle \;=\; b|m\rangle \tag{3.14}$$

with the eigenvalue $E_{m-1} = E_m - \hbar\nu$. There is, however, a lower boundary, as kinetic and potential energies are positive quantities and the eigenvalues cannot

be negative. It is possible to describe the lowest or ground state, as $|0\rangle$ and suppose that the only reliable solution to $Hb|0\rangle = (E_m - \hbar\nu)b|0\rangle$ is

$$b|0\rangle \;=\; 0\,. \tag{3.15}$$

Since there are no lower eigenstates then the ground state. The Schrödinger equation in this scenario recognises,

$$\hbar\nu\left(b^\dagger b + \frac{1}{2}\right)|0\rangle \;=\; \frac{1}{2}\hbar\nu|0\rangle = E_0|0\rangle\,, \tag{3.16}$$

which demonstrates that the energy of the ground state $|0\rangle$ is $E_0 = \frac{1}{2}\hbar\nu$. As a consequence, the whole spectrum of energies follows,

$$E_m \;=\; \hbar\nu\left(m + \frac{1}{2}\right)\,, \tag{3.17}$$

where m is a positive integer or zero. The quantum number m thus indicates the energy level of the harmonic oscillator or in other words the number of energy quanta it possesses. Throughout the rest of this thesis, if the harmonic oscillator is used to describe the vibrational energy of a particle, we shall refer to the energy quanta as phonons.

The role of the ladder operators b and $b^\dagger$ in shifting the energy of the system by the amount of $\hbar\nu$ is indicated in Figure 3.1. The eigenstates of the Hamiltonian in Eq. (3.5) are simultaneous eigenstates to the number operator $b^\dagger b$ and it's obvious from the Eqs. (3.7) and (3.17) that they satisfy

$$b^\dagger b|m\rangle \;=\; m|m\rangle\,. \tag{3.18}$$

The states $|m\rangle$ are the number states or Fock states. It is better to normalise the eigenstates so that

$$\langle m|m\rangle \;=\; 1\,. \tag{3.19}$$

If the states are normalised, we need to modify their relationships. Eq. (3.14) can be generalised to

$$b|m\rangle \;=\; C|m-1\rangle\,, \tag{3.20}$$

Where C an arbitrary constant. If we consider taking the Hermitian conjugate of both sides, that means

$$\langle m|b^\dagger = \langle m-1|C^* \,. \tag{3.21}$$

Multipling Eqs. (3.20) and (3.21) indicates that

$$\begin{aligned} \langle m|b^\dagger b|m\rangle &= |C^2|\langle m-1|m-1\rangle \,, \\ m &= |C^2| \,. \end{aligned} \tag{3.22}$$

The phase of the normalisation constant is usually considered to be zero and Eq. (3.20) becomes

$$b|m\rangle = \sqrt{m}|m-1\rangle \,. \tag{3.23}$$

In analogy, it can be shown that

$$b^\dagger|m\rangle = \sqrt{m+1}|m+1\rangle \,. \tag{3.24}$$

It is worth noting that the condition of ground state (3.15) is included as a special case in Eq.(3.23). Eqs. (3.23) and (3.24) are always better to use than Eqs.(3.12) and (3.14) because of the normalisation. The various energy eigenstates are orthogonal, so that the only non-vanishing matrix elements of operators b and $b^\dagger$ are those of the form

$$\begin{aligned} \langle m-1|b|m\rangle &= \sqrt{m} \,, \\ \langle m+1|b^\dagger|m\rangle &= \sqrt{m+1} \,. \end{aligned} \tag{3.25}$$

Along with Eq. (3.2), this demonstrates that the eigenstates follow the orthonormality condition

$$\langle m|n\rangle = \delta_{mn} \,, \tag{3.26}$$

where δ_{mn} is the Kronecker delta. In terms of Eqs.(3.25), we can see straight away that operators b and $b^\dagger$ are not Hermitian, even though every Hermitian operator A satisfies

$$\langle i|A|j\rangle = \langle j|A|i\rangle^* \tag{3.27}$$

with respect to arbitrary states $|i\rangle$ and $|j\rangle$. However, it is worth noting that operators b and $b^\dagger$ do not represent quantities that can be physically observed. The convenience and representation of the algebra of the ladder operators in many areas of quantum mechanics is highly appreciated.

3.3 Thermalisation of an atomic gas with elastic collisions

In this section, we discuss a possible realisation of the thermalisation stages. More concretely, we assume in the following that elastic collisions transfer the atomic gas into its thermal state. It is shown that this re-distributes energy between all the different vibrational modes of the atoms. For simplicity, we assume here that the atoms do not see the cooling laser during thermalisation stages.

3.3.1 The thermal state of a single harmonic oscillator

We first consider a single trapped atom inside a harmonic trapping potential. Its thermal state equals (Blaise & Henri-Rousseau (2011))

$$\rho = \frac{1}{Z}\,\mathrm{e}^{-\beta H} \qquad \text{with} \qquad Z = \mathrm{Tr}(\mathrm{e}^{-\beta H})\,, \tag{3.28}$$

where H is the relevant harmonic oscillator Hamiltonian, $\beta = 1/k_{\mathrm{B}}T$ is the thermal Lagrange parameter for a given temperature T, k_{B} is Boltzmann's constant and Z denotes the partition function which normalises the density matrix ρ of the atom. For sufficiently large atomic transition frequencies ω_0, the thermal state of the atom is to a very good approximation given by its ground state $|\mathrm{g}\rangle$, unless the atom becomes very hot. In the following, we therefore neglect its electronic degrees of freedom. Hence the Hamiltonian H in Eq. (3.28) equals

$$H \;=\; \hbar\nu\left(b^\dagger b + \tfrac{1}{2}\right)\,, \tag{3.29}$$

where ν and b denote again the frequency and the annihilation operator of a single phonon. Combining Eqs. (3.28) and (3.29), we find that (Blaise & Henri-Rousseau (2011))

$$Z \;=\; \frac{\mathrm{e}^{-\frac{1}{2}\lambda}}{1-\mathrm{e}^{-\lambda}} \tag{3.30}$$

with $\lambda = \beta\hbar\nu$. Here we are especially interested in the expectation value of the thermal energy of the vibrational mode of the trapped atom which equals $\langle H\rangle = \mathrm{Tr}(H\rho)$. Hence using Eqs. (3.28) and (3.29), one can show that

$$\langle H\rangle \;=\; \frac{1}{Z}\mathrm{Tr}\left(H\mathrm{e}^{-\beta H}\right) = -\frac{1}{Z}\frac{\partial}{\partial\beta}Z = -\frac{\partial}{\partial\beta}\ln Z\,. \tag{3.31}$$

Finally, combining this result with Eq. (3.30), we find that

$$\langle H \rangle \;=\; \hbar\nu \left(\frac{\mathrm{e}^{-\lambda}}{\mathrm{e}^{-\lambda}-1} + \frac{1}{2} \right) \tag{3.32}$$

which is Planck's expression for the average energy of a single quantum harmonic oscillator. Moreover,

$$m \;=\; \frac{\mathrm{e}^{-\lambda}}{\mathrm{e}^{-\lambda}-1}\,, \tag{3.33}$$

since the mean phonon number $m = \langle b^\dagger b \rangle$ relates to $\langle H \rangle$ via $m = \langle H \rangle / \hbar\nu - \frac{1}{2}$.

3.3.2 The thermal state of many atoms with collisions

Next we calculate the thermal state of a strongly confined atomic gas with strong elastic collisions. This situation has many similarities with the situation considered in the previous subsection. The atoms constantly collide with their respective neighbours which further increases the confinement of the individual particles. Hence we assume in the following that the atoms no longer experience the phonon frequency ν but an increased phonon frequency ν_{eff}. If all atoms experience approximately the same interaction, their Hamiltonian H equals

$$H \;=\; \sum_{i=1}^{N} \hbar \left(\nu_{\mathrm{eff}} + \tfrac{1}{2} \right) b_i^\dagger b_i \tag{3.34}$$

to a very good approximation. Here b_i denotes again the phonon annihilation operator of atom i. Comparing this Hamiltonian with the harmonic oscillator Hamiltonian in Eq. (3.29) and substituting H in Eq. (3.34) into Eq. (3.28) to obtain the thermal state of many atoms, we find that this thermal state is simply the product of the thermal states of the individual atoms. All atoms have the same thermal state, their mean phonon number $m_i = \langle b_i^\dagger b_i \rangle$ equals

$$m_i \;=\; \frac{\mathrm{e}^{-\lambda_{\mathrm{eff}}}}{\mathrm{e}^{-\lambda_{\mathrm{eff}}}-1} \tag{3.35}$$

with $\lambda_{\mathrm{eff}} = \hbar\nu_{\mathrm{eff}}/k_{\mathrm{B}}T$, in analogy to Eq. (3.33). This equation shows that any previously depleted collective vibrational mode of the atoms becomes re-populated during thermalisation stages.

3.4 Summary

This chapter has focused our attention on the theoretical fact that we covered the theory of a harmonic oscillator in the quantisation. The energy transfer between the states is represented by ladder operators b and $b^\dagger$, and the system's eigenstates are represented by number states $|m\rangle$. The treatment of a harmonic oscillator becomes relatively simple and straightforward using this formalism. The harmonic oscillator is used to define the vibrational energy levels of trapped particles (called phonons) and the energy levels of a radiation mode (called photons). When dealing with trapped atomic systems in cavity-mediated cooling and sonoluminescence, we'll rely heavily on these explanations.

We examined a possible implementation of the thermalisation stages in greater detail. More precisely, the following assumes that elastic collisions convert the atomic gas to its thermal state. It is demonstrated that this re-distributes energy between all of the atoms' different vibrational modes. We have looked not only at the theory of harmonic oscillator eigenstates but also at mixed states that arise when a harmonic oscillator is placed in a thermal equilibrium. In considering canonical density operators, we derived thermal average expressions from the number operator $b^\dagger b$.

Chapter 4

Sonoluminescence

4.1 Introduction

This chapter concentrates on sonoluminescence which is the fascinating phenomenon of strong light flashes of small air bubbles in a fluid. The bubbles are driven by an ultrasonic wave and need to be filled with noble gas atoms. The approximation of the radiation from the emission of blackbody indicates very high temperatures. Although sonoluminescence is studied extensively, there is still some controversy about the origin of the sudden energy level in the bubble collapse phase.

In what follows, we first introduce a brief history of sonoluminescence in section 4.2. The dynamics of the bubbles will be described in a more intuitive way in Section 4.3. A proposed heating mechanism is outlined in Section 4.4.

4.2 A brief history of sonoluminescence

Frenzel & Schultes (1934) discovered by accident a phenomenon which was later described as multi-bubble sonoluminescence (McNamara *et al.* (1999); Walton & Reynolds (1984)). They used ultrasonic waves in a tank with a photographic flow to speed up the development process of the photographs. The results were small imploding bubbles that emit low intensity light (Gaitan *et al.* (1992)) were able to produce a single bubble cavitation. Interest in this phenomenon increased

again in 1989. They created a stable bubble with a periodic change in radius to optimise the experimental setup. The bubble collapses suddenly in each cycle and emits a clear pulse of light. The phenomenon in its new form was called the single-bubble sonoluminescence. Later, these experiments were perfected by the Putterman group [Barber & Putterman (1991, 1992); Camara *et al.* (2004); Hiller *et al.* (1992, 1994, 1998); Vazquez *et al.* (2001, 2002)] , Suslick Eddingsaas & Suslick (2007); Flannigan & Suslick (2005, 2006, 2007); Flint & Suslick (1991)and others (Burdin *et al.* (1999); Ciawi *et al.* (2006); Hilgenfeldt *et al.* (1998, 2000); Lauterborn & Koch (1987); Lee *et al.* (2005); Rae *et al.* (2005); Tsochatzidis *et al.* (2001)). Luminescence of a cavitating bubble was even caused by pulsed laser excitation (Ohl *et al.* (1998)).

4.3 Sonoluminescence

In Gaitan & Crum (1990a) and Gaitan & Crum (1990b), sonoluminescence was initially reported. The width of the light pulse measured by Barber & Putterman (1991) was less than $50\,ps$. This results showed that the light emission is cut off from the bubble dynamics of the single-bubble sonoluminescence. While the classical Rayleigh-Plesset equation can explain the radius of the bubble, the light emission mechanism remains unknown(Brenner *et al.* (2002); Flannigan & Suslick (2007); Suslick & Flannigan (2008)). A sensitive light-emitting dependence on the type of gas in the cavity has also been found (Brenner *et al.* (2002); Hiller *et al.* (1994)). A valuable theoretical model has to take these two phenomena into account, which are not yet classically described.

4.3.1 Single-bubble sonoluminescence

There are two different classes of sonoluminescence: multi-bubble (Frenzel & Schultes (1934); Walton & Reynolds (1984)) and single-bubble sonoluminescence (Brenner *et al.* (2002); Gaitan *et al.* (1992)). Under appropriate situations, a bubble can be balanced by the acoustic force, with acoustic levitation holding a bubble stable in the liquid. Typically, such a bubble is quite small compared

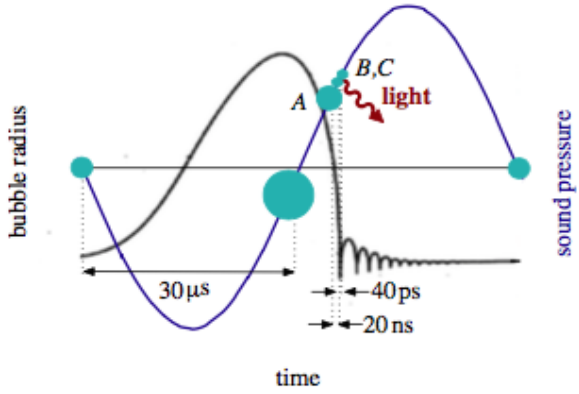

Figure 4.1: Time dependence of typical single-bubble sonoluminescence cycle depends on driving the sound pressure and bubble radius. Point A is the start of the collapse phase in which the bubble is insulated thermally from the liquid. At point B, the bubble has considerably higher temperatures and there is a strong light flash. Point C refers to the beginning of the expansion phase in which the bubble wavers over its balance radius until its stability recovers.

to an acoustic wavelength and can contain the trapped van der Waals gas's particles close to their covolumes. A single, stable, oscillating gas bubble can be driven into large amplitude pulsations under special conditions, which produce sonoluminescence during each acoustic cycle.

Fig. 4.1 illustrates a typical single-bubble sonoluminescence cycle and shows the corresponding time scales. Bubble acts isothermically most of the cycle. The applied sound wave takes approximately $60\mu s$. Dependence of time on the bubble radius is well in accordance with the law of classical physics and can be presented in the equations of Rayleigh-Plesset (Moss (1997)). The bubble radius increases isothermally over most of the cycle. A quick collapse follows every expansion stage. The accelerating bubble wall becomes so fast, near point A, about $20\,ns$ before the minimum radius is reached, that the liquid is thermally isolated. The bubble may be filled with up to 10^8 noble gas atoms close to its minimum radius of about $0.5d\mu m$, i.e. between points B and C. At this point, the energy density is rapidly increased with the sudden light emission. The light flash lasts approximately $40\,ps$ in case of Argon atoms. Then begins a phase of

re-expansion in which the bubble oscillate in its balance radius until it regains stability.

4.3.2 Cavitation Heats up

In point B, the bubble's temperature rises significantly with a heating rate of $10^{10} - 10^{11}\, K/s$ and a strong light flash which lasts around $40\, ps$. Detailed picosecond light flash spectra measurements have been carried out between the points B and C of Fig. 4.1. The association with the radiation of black body or Bremsstrahlung radiation of the continuum underlying these sound light spectrums indicates a minimum temperature of $10^3 - 10^4$ K within the bubble (Barber & Putterman (1991); Didenko *et al.* (2000); Hiller *et al.* (1992); Suslick & Flannigan (2008); Vazquez *et al.* (2001, 2002)). Light emissions in the ultraviolet regime can even be observed, which indicate about $10^6\, K$ in temperatures (Camara *et al.* (2004)). It is worth noting that the optical regime has discovered strong emission lines (Brenner *et al.* (2002); Flannigan & Suslick (2007); Suslick & Flannigan (2008)). These indicate the population of highly energised, thermally unpopulated noble gas (Eddingsaas & Suslick (2007); Flannigan & Suslick (2005, 2006))and metal atoms (Flannigan & Suslick (2007)). These excitations demonstrate the development of the opaque plasma core within the bubble and were observed in multiple experiments on the single and the multi-bubble sonoluminescence(Didenko & Gordeychuk (2000); Eddingsaas & Suslick (2007); Suslick & Flannigan (2008)). There has already been a dense plasma within the bubble in recent experiments (Eddingsaas & Suslick (2007); Flannigan & Suslick (2005, 2006)).

4.3.3 Sonoluminescence light emission

Because of their instability, the spectra are less reproducible in multi-bubble sonoluminescence experiments than the spectra in single-bubble sonoluminescence. The light pulse is almost Gaussian in single-bubble sonoluminescence experiment and contains a broad range of frequencies (Gompf *et al.* (1997)). The pulse width and emission time have been confirmed to be indicative of the wavelength of the light emitted (Hiller *et al.* (1998)). The temperature inside the bubble is generally assumed to increase by thousands of kelvin during the phase

of compression, and the collapse of the bubble phase creates conditions for plasma formation. The light flash at the end of the bubble collapse phase has been attributed to surface blackbody radiation (Hiller *et al.* (1992); Hopkins *et al.* (2005); Vazquez *et al.* (2001, 2002)). Neutral and ion Bremsstrahlung (Moss (1997); Moss *et al.* (1999); Wu & Roberts (1993); Xu *et al.* (1998)), collision-induced emission (Frommhold (1998); Frommhold & Atchley (1994)), quantum vacuum radiation (Didenko & Gordeychuk (2000); Schwinger (1992)), and other thermal (Hilgenfeldt *et al.* (1999a,b); Hiller *et al.* (1998)) as well as non-thermal processes have been considered (cf. Bernstein & Zakin (1995); Garcia & Levanyuk (1996); Willison (1998)). Other authors assume a converging spherical shock wave in the bubble's plasma temperature (Moss *et al.* (1994); Wu & Roberts (1993)). All these models qualitatively replicate the observed sonoluminescence spectra with a single bubble. However, most of them fail to predict the independent width and emission time of the wavelength.

4.4 Quantum optical heating in sonoluminescence experiments

This section focuses on a quantum optical heating mechanism in sonoluminescence experiments. A quantum optical heating mechanism is discussed which might contribute substantially to the sudden energy concentration in sonoluminescence experiments. As mentioned earlier, a typical single-bubble sonoluminescence cycle is illustrated in Fig. 4.1. The bubble reaches a critical radius as it expands, at which point it rapidly collapses. The collapse is accompanied by a flash of light, indicating extremely high temperatures inside the bubble. The bubble oscillates around its equilibrium radius afterward until it regains stability.

The emission of light consists primarily of a continuum of radiation from black body or Bremsstrahlung radiation. Detailed light spectrum measurements show temperatures above 10^4 K (Barber & Putterman (1991); Hiller *et al.* (1992); Vazquez *et al.* (2001)). Light emitting in the ultraviolet mode can even be noted, which suggests a bubble driven at $1MHz$ at temperatures of around 10^6 K (Camara *et al.* (2004)). Transition line emissions from high energy noble gas atomic

states which cannot be thermally populated (Flannigan & Suslick (2005, 2007)) point to an opaque plasma core formation (Suslick & Flannigan (2008)) . There has also been evidence of a plasma core in sonoluminescence experiments with multiple bubble (Eddingsaas & Suslick (2007)).

The theoretical understanding of the time dependence on the bubble radius and its virtually adiabatic compression is certain when the minimum radius approaches (Brenner *et al.* (2002); Suslick & Flannigan (2008)). It remains controversial what is the condition of the bubble during the last part of the collapse phase and the conditions leading to these huge heating rates to very high temperatures. Here we summarise the notion that heating occurs during fast bubble deformations due to the presence of a highly inhomogeneous electrical field (Kurcz *et al.* (2009b)). This field establishes a coupling between the movement of the noble atoms and their electronic freedom. A quantum optical heating process may occur when combined with spontaneous emissions from the atoms. The cooling of ion trap experiment is based on very similar couplings (Leibfried *et al.* (2003a)).

4.4.1 The basic mechanism

In this subsection, we explain the basic idea behind the considered quantum optical heating mechanism, essentially following the discussion in (Kurcz *et al.* (2009a,b)). The bubble is no longer in thermal equilibrium as it approaches its minimum radius close to point B in Fig. 4.1. Suddenly, entropy increases and the processes are highly irreversible. This causes a higher temperature than thermodynamic heating processes can be causing (see Fig. 4.1). We answer two questions in the following: Why do noble gas atoms have to fill the bubbles? What is the main mechanism for focusing energy during the bubble collapse?

Near point B, the mean distance between noble gas atoms is so small that Lennard-Jones potential can describe interactions between them. Indeed, a solid state system becomes the physical condition of the bubble. The atoms are balanced by the van der Waals interaction between repulsive, interatomic forces, because the orbitals overlap and the attractive forces. Any significant temperature increase must therefore be driven by vibrational motion into the quantum regime. The generation of light also requires an open quantum system.

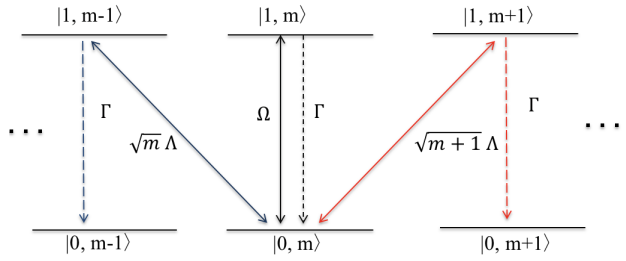

Figure 4.2: Level configuration of a single atom-phonon system which demonstrates the immediate transitions when the atom is in its ground state initially $|0\rangle$ and exactly has m phonons. Ω represents the coupling constant for phonon conserving transitions to the excited atomic state $|1\rangle$, while Λ is a coupling between the electronic and the motional states of the atom. In addition, Γ denotes the level 1 spontaneous photon decay rate.

To model the resulting strong confinement of the atoms, we put each of these into an approximately harmonic trapping potential. It allows us to quantize the atomic motion just before maximum compression of the bubble during the collapse phase. In this regard, phonons with frequency ν are able to describe the motion states of each atom.

To simplify this, we suppose that atoms are effective two level systems with ground state $|0\rangle$ and excited state $|1\rangle$. The relating interaction Hamiltonian contains terms that cause the excitation and de-excitation of each atom, followed by the creation and the annihilation of a phonon. Also important is the presence of a large spontaneous decay rate Γ of the excited state $|1\rangle$ that maintains the atoms in their ground state. While these processes are very non-resonant, the mean phonon number is changed considerably per atom and the temperature in the bubble increases even in a few nanoseconds, by many orders of magnitude.

We therefore consider intuitive description of the proposed heating mechanism. Assume that an atom is in its ground state initially and has m phonons, this state is marked by $|0, m\rangle$, as shown in Fig. 4.2. It is worth noting that phonons are bosons with respect to their annihilation and creation operator b

and $b^\dagger$. Hence, as we have seen in the previous section,

$$\begin{aligned} b &= \sum_{m=0}^{\infty} \sqrt{m}|m-1\rangle\langle m|\,, \\ b^\dagger &= \sum_{m=0}^{\infty} \sqrt{m+1}|m+1\rangle\langle m|\,, \end{aligned} \tag{4.1}$$

with the usual bosonic commutator relation $[b, b^\dagger] = 1$.

As a result, a transition from the state $|0, m\rangle$ to the $|1, m+1\rangle$ takes place with a rate proportional to $\sqrt{m+1}$, whereas the rate for a transition from $|0, m\rangle$ to $|1, m-1\rangle$ scales as $\sqrt{m}$. Since the atomic spontaneous decay rate is relatively large, the most likely result of such a transition is a non-reversible and primarily non-radiative transition into the atomic ground state. This transfers the atom to either its initial state $|0, m\rangle$, into $|0, m-1\rangle$, or into $|0, m+1\rangle$. Since the final population in the state with $m+1$ phonons is greater than the state population with $m-1$ phonons, the net impact of the presented excitation and de-excitation process are to increase the mean number of phonon by atom, that is, heating.

4.4.2 Single bubble sonoluminescence experiments

Sonoluminescence can be defined as a phenomenon of strong light emission from collapsing bubbles in a liquid, like water (Brenner *et al.* (2002); Camara *et al.* (2004); Gaitan *et al.* (1992)). As mentioned above, these bubbles need to be filled with noble gas atoms which occur naturally in air. Alternatively, the bubbles can be filled with ions from ionic liquids, molten salts, and concentrated electrolyte solutions (Flannigan *et al.* (2005)). Moreover, the bubbles need to be acoustically confined and periodically driven by ultrasonic frequencies. As a result, the bubble radius changes periodically in time, as illustrated in Fig. 4.3. The oscillation of the bubble radius regenerates itself with unusual precision.

At the beginning of every expansion phase, the bubble oscillates about its equilibrium radius until it returns to its stability. During this process, the bubble temperature changes adiabatically and there is an exchange of thermal energy between the atoms inside the bubble and the surrounding liquid. During the collapse phase of a typical single-bubble sonoluminescence, i.e. when the bubble reaches

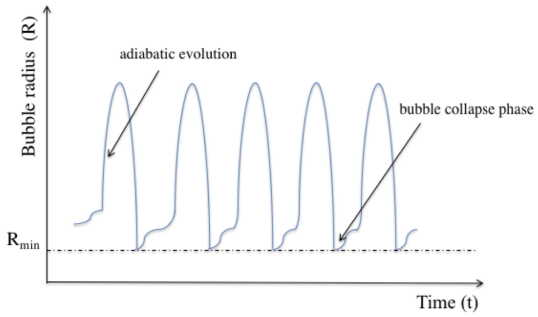

Figure 4.3: Schematic view of the time dependence of the bubble radius in a typical single-bubble sonoluminesence experiment. Most of the time, the bubble evolves adiabatically and exchanges thermal energy with its surroundings. However, at regular time intervals, the bubble radius suddenly collapses. At this point, the bubble becomes thermally isolated. When it reaches its minimum radius, the system usually emits a strong flash of light in the optical regime.

its minimum radius, its inside becomes thermally isolated from the surrounding environment and the atomic gas inside the bubble becomes strongly confined. Usually, a strong light flash occurs at this point which is accompanied by a sharp increase of the temperature of the particles. Experiments have shown that increasing the concentration of atoms inside the bubble increases the intensity of the emitted light (Flannigan & Suslick (2005); Suslick & Flannigan (2008)). All these observations are in good agreement with the heating mechanism described in previous subsection.

4.4.3 A quantum optics perspective on sonoluminescence

The above observations suggest many similarities between sonoluminescence and quantum optics experiments with trapped atomic particles (Beige & Kim (2015a); Kurcz *et al.* (2009b)). When the bubble reaches its minimum radius, an atomic gas becomes very strongly confined (Moss (1997)). The quantum character of the atomic motion can no longer be neglected and, as in ion trap experiments (cf. Section 2.1.3), the presence of phonons with different trapping frequencies ν

has to be taken into account. Moreover, when the bubble reaches its minimum radius, its surface can become opaque and almost metallic (Khalid *et al.* (2012)). When this happens, the bubble traps light inside and closely resembles an optical cavity which can be characterised by a frequency ω_{cav} and a spontaneous decay rate κ. Since the confined particles have atomic dipole moments, they naturally couple to the quantised electromagnetic field inside the cavity. The result can be an exchange of energy between atomic dipoles and the cavity mode. The creation of photons inside the cavity is always accompanied by a change of the vibrational states of the atoms. Hence the subsequent spontaneous emission of light in the optical regime results in a permanent change of the temperature of the atomic particles.

A main difference between sonoluminescence and cavity-mediated collective laser cooling is the absence and presence of external laser driving (cf. Section 2.2.4). But even in the absence of external laser driving, there can be a non-negligible amount of population in the excited atomic states $|\mathrm{e}\rangle$. This applies, for example, if the atomic gas inside the cavitating bubble is initially prepared in the thermal equilibrium state of a finite temperature T. Once surrounded by an optical cavity, as it occurs during bubble collapse phases, excited atoms can return into their ground state via the creation of a cavity photon (cf. Fig. 4.4). Suddenly, an additional de-excitation channel has become available to them. As pointed out in Refs. Beige & Kim (2015a); Kurcz *et al.* (2009b), the creation of a cavity photons is more likely accompanied by the creation of a phonon than the annihilation of a phonon since

$$\begin{aligned} B^{\dagger} &= \sum_{m=0}^{\infty} \sqrt{m+1}\,|m+1\rangle\langle m|\,, \\ B &= \sum_{m=0}^{\infty} \sqrt{m}\,|m-1\rangle\langle m|\,. \end{aligned} \tag{4.2}$$

Here B and $B^{\dagger}$ denote the relevant phonon annihilation and creation operators, while $|m\rangle$ denotes a state with exactly m phonons. As one can see from Eq. (4.2), the normalisation factor of $B^{\dagger}\,|m\rangle$ is slightly larger than the normalisation factor of the state $B\,|m\rangle$. When the cavity photon is subsequently lost via spontaneous photon emission, the newly-created phonon remains inside the bubble. Hence the

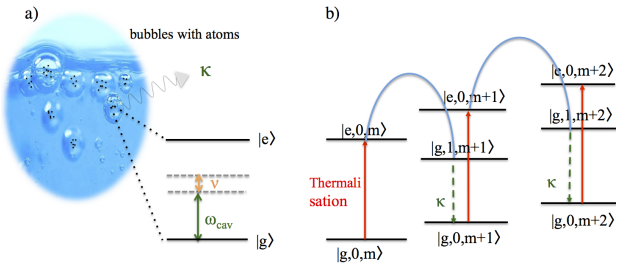

Figure 4.4: (a) From a quantum optics point of view, one of the main characteristics of sonoluminescence experiments is that cavitating bubbles provide a very strong confinement for atomic particles. This means, the quantum character of their motional degrees of freedom has to be taken into account. As in ion trap experiments, we denote the corresponding phonon frequency in this chapter by ν. Moreover, during its collapse phase, the surface of the bubble becomes opaque and confines light, thereby forming an optical cavity with frequency ω_{cav} and a spontaneous decay rate κ. (b) Even in the absence of external laser driving, some of the atoms are initially in their excited state $|\mathrm{e}\rangle$ due to being prepared in a thermal equilibrium state at a finite temperature T. When returning into their ground state via the creation of a cavity photon which is only possible during the bubble collapse phase, most likely a phonon is created. This creation of phonons implies heating. Indeed, sonoluminescence experiments often reach relatively high temperatures (Flannigan & Suslick (2005); Suslick & Flannigan (2008)).

light emission during bubble collapse phases is usually accompanied by heating, until the sonoluminescing bubble reaches an equilibrium.

During each bubble collapse phase, cavitating bubbles are thermally isolated from their surroundings. However, during the subsequent expansion phase, system parameters change adiabatically and there is a constant exchange of thermal energy between atomic gas inside the bubble and the surrounding liquid (cf. Fig. 4.3). Eventually, the atoms reach an equilibrium between heating during bubble collapse phases and the loss of energy during subsequent expansion phases. Experiments have shown that the atomic gas inside the cavitating bubble

can reach temperature of the order of 10^4 K which strongly supports the hypothesis that there is a very strong coupling between the vibrational and the electronic states of the confined particles (Flannigan & Suslick (2005); Suslick & Flannigan (2008)).

4.5 Summary

In this chapter, we provided a basic introduction to the sonoluminescence phenomenon. As well as this, we identified main heating properties of sonoluminescence of single cavitating bubbles. A quantum optical heating mechanism has been described which may make a significant contribution to the sudden energy level of the sonoluminescence experiments. The basic idea behind the considered quantum optical heating mechanism was explained. The reason for heating stage is that phonon creating processes are more likely than phonon annihilating processes.

As we shall see later, the thermalisation stage and the heating stage are closely linked and both need to explain the sonoluminescence cycle. Heating takes place during a lifecycle collapse phase, followed by an expanding phase of growth during which the bubble radius gradually increases. During the collapse, the bubble wall becomes opaque and within the radiation field closely resembles an optical cavity. In an optical cavity, we treat the atomic system trapped inside the bubble, whilst the collapse was modelled on the quantum optical approach.

Part 2: New results

Chapter 5

A quantum heat exchanger for nanotechnology: Motivation and basic ideas

5.1 Introduction

The main purpose of this chapter is to design a quantum heat exchanger which converts heat into light on relatively short quantum optical time scales. Our scheme takes advantage of heat transfer as well as collective cavity-mediated laser cooling of an atomic gas inside a cavitating bubble. Laser cooling routinely transfers individually trapped ions to nano-keflvin temperatures for applications in quantum technology. The quantum heat exchanger which we propose here might be able to provide cooling rates of the order of kelvin temperatures per millisecond and is expected to find applications in micro and nanotechnology.

In this chapter, we ask the question whether laser cooling could also have applications in micro and nanoscale physics experiments. For example, nanotechnology deals with objects which have dimensions between 1 and 1000 nanometers and is well known for its applications in information and communication technology, as well as sensing and imaging. Increasing the speed at which information can be processed and the sensitivity of sensors is usually achieved by reducing system dimensions. However, smaller devices are usually more prone to heating as thermal resistances increase (Hsu (2008)). Sometimes, large surface to volume

ratios can help to off-set this problem. Another problem for nanoscale sensors is thermal noise. As sensors are reduced in size, their signal to noise ratio usually decreases and thus the thermal energy of the system can limit device sensitivity (Kim *et al.* (2001)). Therefore thermal considerations have to be taken into account and large vacuums or compact heat exchangers have already become an integral part of nanotechnology devices.

Usually, heat exchangers in micro and nanotechnology rely on fluid flow (Saniei (2007)). In this chapter, we propose an alternative approach. More concretely, we propose to use heat transfer as well as a variation of laser cooling, namely cavity-mediated collective laser cooling (Beige *et al.* (2005); Domokos & Ritsch (2002); Kim *et al.* (2018); Ritsch *et al.* (2013)). As illustrated in Fig. 5.1, the proposed quantum heat exchanger mainly consists of a liquid which contains a large number of cavitating bubbles filled with noble gas atoms. Transducers constantly change the radius of these bubbles which should resemble optical cavities when they reach their minimum radius during bubble collapse phases. At this point, a continuously applied external laser field rapidly transfers vibrational energy of the atoms into light. If the surrounding liquid contains many cavitating bubbles, their surface area becomes relatively large and there can be a very efficient exchange of heat between the inside and the outside of cavitating bubbles. Any removal of thermal energy from the trapped atomic gas inside bubbles should eventually result in the cooling of the surrounding liquid and of the surface area of the device on which it is placed.

In this chapter, we emphasise that cavitating bubbles can provide all of the requirements (1) − (3) for laser cooling which we listed earlier in this thesis in chapter 2, especially, a very strong confinement of atomic particles, like nitrogen (Beige & Kim (2015a); Kurcz *et al.* (2009b); Moss (1997)). In addition, the surfaces of cavitating bubbles can become opaque during the bubble collapse phase (Khalid *et al.* (2012)), thereby creating a spherical optical cavity (Daul & Grangier (2005a,b))which is an essential requirement for cavity-mediated collective laser cooling. To initiate the cooling process, an appropriately detuned laser field needs to be applied in addition to the transducers which confine the bubbles with sound waves. Although sonoluminescence has been studied in great detail and the idea of applying laser fields to cavitating bubbles is not new (Cao *et al.*

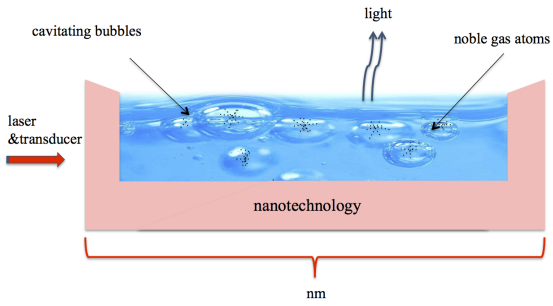

Figure 5.1: Schematic view of the proposed quantum heat exchanger. It consists of a liquid in close contact with the area which we want to cool. The liquid should contain cavitating bubbles which are filled with atomic particles, like Nitrogen, and should be driven by sounds waves and laser light. The purpose of the sound waves is to constantly change bubble sizes. The purpose of the laser is to convert thermal energy during bubble collapse phases into light.

(2008)), not enough is known about the relevant quantum properties, like phonon frequencies. Hence we cannot predict realistic cooling rates for the experimental setup shown in Fig. 5.1. However, a crude estimate which borrows data from different, already available experiments suggests that it might be possible to achieve cooling rates of the order of Kelvin temperatures per millisecond for volumes of liquid on a cubic micrometer scale.

Sonoluminescence experiments are well-known for converting sound into relatively large amounts of thermal energy, while producing light in the optical regime (Brenner *et al.* (2002); Camara *et al.* (2004); Gaitan *et al.* (1992)). During this process, the atomic gas inside a cavitating bubbles can reach very high temperatures (Flannigan & Suslick (2005); Flannigan *et al.* (2005)). These hint at the presence of a very strong coupling between the electronic and the vibrational degrees of freedom of the atomic gas. Moreover, cavitating bubbles already have applications in sonochemistry, where they are used to provide energy for chemical reactions (Suslick (1990)). Here we propose to exploit the atom-phonon interactions in sonoluminescence experiments for laser cooling of solid state systems. As we shall see below, in the presence of an appropriately detuned laser field, we

expect other, usually present highly-detuned heating processes to become secondary.

There are two sections in this chapter. The purpose of Section 5.2 is to review the main design principles of a quantum heat exchanger for nanotechnology. As we shall see below, this technique is a variation of standard laser cooling techniques for individually trapped atomic particles. We provide an overview of the experimental requirements and estimate achievable cooling rates. Finally, we summarise our findings in Section 5.3.

5.2 A quantum heat exchanger with cavitating bubbles

As pointed out in Section 5.1, the aim of this chapter is to design a quantum heat exchanger for nanotechnology. The proposed experimental setup consists of a liquid on top of the device which we aim to keep cool, a transducer and a cooling laser (cf. Fig. 5.1). The transducer generates cavitating bubbles which need to contain atomic particles and whose diameters need to change very rapidly in time. The purpose of the cooling laser is to stimulate the conversion of heat into light. The cooling of the atomic particles inside cavitating bubbles subsequently aids the cooling of the liquid which surrounds the bubbles and its environment via adiabatic heat transfers.

To gain a better understanding of the experimental setup in Fig. 5.1, Section 4.4.2 describes the main characteristics of single bubble sonoluminescence experiments (Brenner *et al.* (2002); Camara *et al.* (2004); Flannigan & Suslick (2005); Flannigan *et al.* (2005); Gaitan *et al.* (1992)). Section 4.4.3 emphasises that there are many similarities between sonoluminescence and quantum optics experiments (Beige & Kim (2015a); Kurcz *et al.* (2009b)). From this we conclude that sonoluminescence experiments naturally provide the main ingredients for the implementation of cavity-mediated collective laser cooling of an atomic gas (Beige *et al.* (2005); Kim *et al.* (2018)). Finally, in Sections 5.2.1 and 5.2.2, we describe the physics of the proposed quantum heat exchanger and estimate cooling rates.

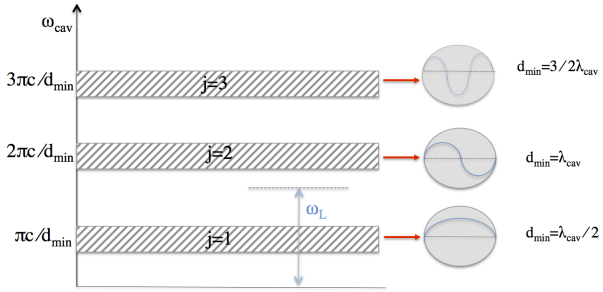

Figure 5.2: When the cavitating bubbles inside the liquid reach their minimum diameters $d_{\min}$, their walls become opaque and trap light on the inside. To a very good approximation, they form cavities which can be described by spontaneous decay rates κ and by cavity frequencies ω_{cav} (cf. Eq. (5.1)). Suppose the diameters of the bubbles inside the liquid occupy a relatively small range of values. Then every integer number j in Eq. (5.1) corresponds to a relatively narrow range of cavity frequencies ω_{cav}. Here we are especially interested in the parameter j for which the ω_{cav}'s lie in the optical regime. When this applies, we can apply a cooling laser with an optical frequency ω_{L} which can cool the atoms in all bubbles. Some bubbles will be cooled more efficiently than others. But as long as the relevant frequency bands are relatively narrow, none of the bubbles will be heated.

5.2.1 Cavity-mediated collective laser cooling of cavitating bubbles

The previous subsection has shown that, during each collapse phase, the dynamics of the cavitating bubbles in Fig. 5.1 is essentially the same as the dynamics of the experimental setup in Fig. 2.2 but with the single atom replaced by an atomic gas. When the bubble reaches its minimum diameter $d_{\min}$, it forms an optical cavity which supports a discrete set of frequencies ω_{cav},

$$\omega_{\text{cav}} \;=\; j \times \frac{\pi c}{d_{\min}}\,, \tag{5.1}$$

where c denotes the speed of light in air and $j = 1, 2, \ldots$ is an integer. As illustrated in Fig. 5.2, the case $j = 1$ corresponds to a cavity photon wavelength $\lambda_{\text{cav}} = 2d_{\min}$. Moreover, $j = 2$ corresponds to $\lambda_{\text{cav}} = d_{\min}$ and so on. Under

realistic conditions, the cavitating bubbles are not all of the same size which is why every j is usually associated with a range of frequencies ω_{cav} (cf. Fig. 5.2). Here we are especially interested in the parameter j, where the relevant cavity frequencies lie in the optical regime. All other parameters j can be neglected, once a laser field with an optical frequency ω_{L} is applied, if neighbouring frequency bands are sufficiently detuned.

In addition we know that the phonon frequency ν of the collective phonon mode B assumes its maximum ν_{max} during the bubble collapse phase. Suppose the cavity detuning $\Delta_{\text{cav}} = \omega_{\text{L}} - \omega_{\text{cav}}$ of the applied laser field is chosen such that

$$\Delta_{\text{cav}} \sim \nu_{\text{max}} \quad \text{and} \quad \nu_{\text{max}} \geq \kappa\,, \tag{5.2}$$

in analogy to Eq. (2.2). As we have seen in Section 2.2.4, in this case, the two-step transition which results in the simultaneous annihilation of a phonon and the creation of a cavity photon becomes resonant and dominates the system dynamics. If the creation of a cavity photon is followed by a spontaneous emission, the previously annihilated phonon cannot be restored and is permanently lost. Overall, we expect this cooling process to be very efficient, since the atoms are strongly confined and cavity cooling rates are collectively enhanced (c.f. Eq. (2.17)).

In order to cool not only very tiny but larger volumes, the experimental setup in Fig. 5.1 should contain a relatively large number of cavitating bubbles. Depending on the quality of the applied transducer, the minimum diameters d_{min} of these bubbles might vary in size. Consequently, the collection of bubbles supports a finite range of cavity frequencies ω_{cav} (cf. Fig. 5.2) so that it becomes impossible to realise the ideal cooling condition $\Delta_{\text{cav}} \sim \nu_{\text{max}}$ in Eq. (5.2) for all bubbles. However, as long as the frequency ω_{L} of the cooling laser is smaller than all optical cavity frequencies ω_{cav}, the system dynamics will be dominated by cooling and not by heating. In general, it is important that the diameters of the bubbles does not vary by too much.

Section 2.2.4 also shows that cavity-mediated collective laser cooling only removes thermal energy from a single collective vibrational mode B of the atoms. Once this mode is depleted, the cooling process stops. To efficiently cool an entire atomic gas, a mechanism is needed which rapidly re-distributes energy between different vibrational degrees of freedom, for example, via thermalisation

based on elastic collisions (cf. Section 3.3). As we have seen above, between cooling stages, cavitating bubbles evolve essentially adiabatically and the atoms experience strong collisions. In other words, the expansion phase of cavitating bubbles automatically implements the intermittent thermalisation stages of cavity-mediated collective laser cooling.

Finally, let us point out that it does not matter, whether the cooling laser is turned on or off during thermalisation stages, i.e. during bubble expansion phases. As long as optical cavities only form during the bubble collapse phases, the above described conversion of heat into light only happens, when the bubble reaches its minimum diameter.The reason for this is that inert gas atoms, like nitrogen, have very large transition frequencies ω_0. The direct laser excitation of atomic particles is therefore relatively unlikely, even when the cooling laser is turned on. If we could excite the atoms directly by laser driving, we could cool them even more efficiently (cf. Section 2.1.3).

5.2.2 Cooling of the surroundings via heat transfer

The purpose of the heat exchanger which we propose here is to constantly remove thermal energy from the liquid surrounding the cavitating bubbles and device on which the liquid is placed (cf. Fig. 5.1). As described in the previous subsection, the atomic gas inside the bubbles is cooled by very rapidly converting heat into light during each collapse phase. Inbetween collapse phases, the cavitating bubbles evolve adiabatically and naturally cool their immediate environment via heat transfer. As illustrated in Fig. 5.3, alternating cooling and thermalisation stages (or collapse and expansion phases) is expected to implement a quantum heat exchanger which does not require the actual transport of particles from one place to another.

Finally, let us have a closer look at achievable cooling rates for micro and nanotechnology devices with length dimensions in the nano and micrometer regime. Unfortunately, we do not know how rapidly heat can be transferred from the nanotechnology device to the liquid and from there to the atomic gas inside the cavitating bubbles. However, any thermal energy which is taken from the atoms

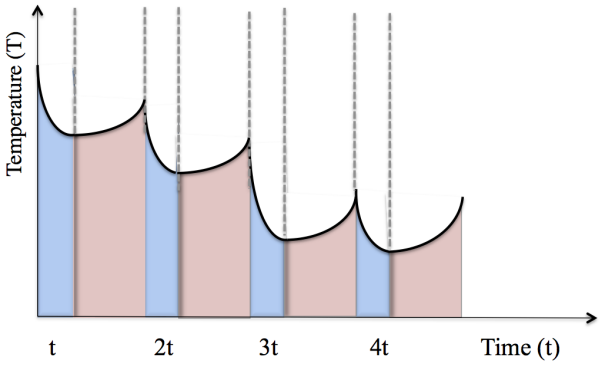

Figure 5.3: Schematic view of the expected dynamics of the temperature of a confined atomic gas during bubble collapse stages (blue) and expansion stages (pink). During expansion stages, heat is transferred from the outside into the inside of the bubble, thereby increasing the temperature of the atoms. During bubble collapse stages, heat is converted into light, thereby resulting in the cooling of the system in Fig. 5.1. Eventually, both processes balance each other out and the temperature of the system remains constant on a coarse grained time scale.

comes eventually from the environment which we aim to cool. Suppose the relevant phonon frequencies $\nu_{\max}$ are sufficiently large to ensure that every emitted photon indicates the loss of one phonon, i.e. the loss of one energy quantum $\hbar\nu_{\max}$. Moreover, suppose our quantum heat exchanger contains a certain amount of liquid, let us say water, of mass m_{water} and heat capacity $c_{\text{water}}(T)$ at an initial temperature T_0. Then we can ask the question, how many photons N_{photons} do we need to create in order to cool the water by a certain temperature ΔT?

From thermodynamics, we know that the change in the thermal energy of the water equals

$$\Delta Q \;=\; c_{\text{water}}(T_0)\, m_{\text{water}} \Delta T \tag{5.3}$$

in this case. Moreover, we know that

$$\Delta Q \;=\; N_{\text{photons}}\, \hbar\nu_{\max}\,. \tag{5.4}$$

Hence the number of photons that needs to be produced is given by

$$N_{\text{photons}} \;=\; \frac{c_{\text{water}}(T_0)\, m_{\text{water}}\, \Delta T}{\hbar\nu_{\max}}\,. \tag{5.5}$$

The time t_{cool} it would take to create this number of photons equals

$$t_{\text{cool}} \quad = \quad \frac{N_{\text{photons}}}{N_{\text{atoms}}\, I}\,, \tag{5.6}$$

where I denotes the average single-atom photon emission rate and N_{atoms} is the number of atoms involved in the cooling process. When combining the above equations, we find that the cooling rate $\gamma_{\text{cool}} = t_{\text{cool}}/\Delta T$ of the proposed cooling process equals

$$\gamma_{\text{cool}} \quad = \quad \frac{c_{\text{water}}(T)\, m_{\text{water}}}{N_{\text{atoms}}\, I\, \hbar \nu_{\text{max}}} \tag{5.7}$$

to a very good approximations.

As an example, suppose we want to cool one cubic micrometer of water ($V_{\text{water}} = 1\,\mu\text{m}^3$) at room temperature ($T_0 = 20\,^0\text{C}$). In this case, $m_{\text{water}} = 10^{-15}\,\text{g}$ and $c_{\text{water}}(T_0) = 4.18\,\text{J/gK}$. Suppose $\nu = 100\,\text{MHz}$ (a typical frequency in ion trap experiments is $\nu = 10\,\text{MHz}$), $I = 10^6/\text{s}$ and $N_{\text{atoms}} = 10^8$ (a typical bubble in single bubble sonoluminescence contains about 10^8 atoms). Substituting these numbers into Eq. (5.6) yields a cooling rate of

$$\gamma_{\text{cool}} \quad = \quad 3.81\,\text{ms}/K\,. \tag{5.8}$$

Achieving cooling rates of the order of kelvin temperatures per millisecond seems therefore experimentally feasible. As one can see from Eq. (5.6), to reduce cooling rates further, one can either reduce the volume that requires cooling, increase the number of atoms involved in the cooling process or increase the trapping frequency ν_{max} of the atomic gas inside collapsing bubbles. All of this is, at least in principle, possible.

5.3 Summary

In this chapter we point out similarities between quantum optics experiments with strongly confined atomic particles and single bubble sonoluminescence experiments (Beige & Kim (2015a,b); Kurcz *et al.* (2009b)). In both situations, interactions are present which can be used to convert thermal energy very efficiently into light. When applying an external cooling laser to cavitating bubbles,

as illustrated in Fig. 5.1, we therefore expect a rapid transfer of heat into light which can eventually result in the cooling of relatively small devices. Our estimates show that it might be possible to achieve cooling rates of the order of milliseconds per Kelvin temperature for cubic micrometers of water. The proposed quantum heat exchanger is expected to find applications in research experiments and in micro and nanotechnology. A closely related cooling technique, namely laser cooling of individually trapped ions, already has a wide range of applications in quantum technology (Barreiro *et al.* (2011); Debnath *et al.* (2016); Leibfried *et al.* (2003b); Ludlow *et al.* (2015); Maiwald *et al.* (2009); Porras & Cirac (2004); Schmidt-Kaler *et al.* (2003); Stephenson *et al.* (2020)). This chapter provided a more qualitative description of a possible quantum heat exchanger. Next we introduced the proposed scheme, while ignoring the presence of an optical cavity for simplicity.

Chapter 6

Laser cooling of indistinguishable particles in cavitating bubbles without cavity formation

6.1 Introduction

Optical cooling of solid state systems, even if it is only of very small volume fractions, would immediately find a wide range of applications in quantum, nano and micro technology. Motivated by this, in Chapter 5, we designed a collective laser-cooling scheme for indistinguishable atoms in cavitating bubbles and showed that these could act as the basic building blocks of quantum heat exchangers (Aljaloud *et al.* (2020)). In this final chapter, we describe the underlying physical processes and provide additional guidance for quantum optics experiments with cavitating bubbles without cavity formation. For simplicity, we assume in the following that the bubbles remain always transparent and show that it is, in principle, possible to transfer an atomic gas inside a cavitating bubble to very low temperatures.

The basic idea of laser cooling for atoms was first started by Hänsch and Schawlow as well as separately for trapped ions by Wineland and Dehmelt (Hänsch & Schawlow (1975); Wineland & Dehmelt (1975); Wineland & Itano (1979)). Considering the light beam holds momentum and energy, a major

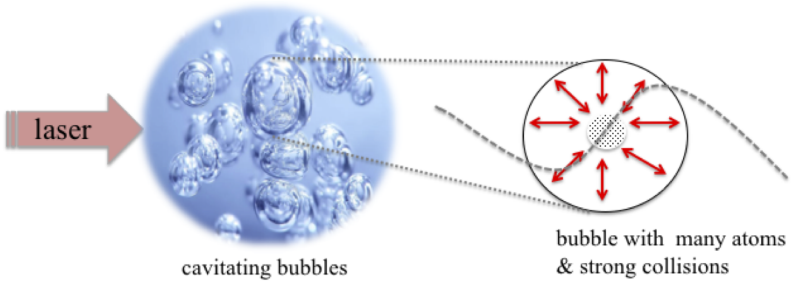

Figure 6.1: Water contains a large number of cavitating bubbles which are filled with atomic particles, like Nitrogen. The water should be driven by sounds waves and laser light. The Bubbles have many atoms with strong collisions.

interesting point is that scattering beam on atoms can consequence considerable changes of the vibrational energy of enormous particles. Over the past few decades, laser cooling techniques have been created which allow for the cooling of atoms to very low temperatures. Applications of these very cold atoms range from testing the foundations of quantum physics to the design of novel quantum technologies. Due to their importance, cooling techniques attract a lot of interest in the literature as we have seen in chapter 2.

Unfortunately, applying a cooling laser to many atoms simultaneously only results in the cooling of a single collective phonon mode of a strongly confined atomic gas. To nevertheless transfer an atomic gas to very low temperatures, i.e. to remove phonons from all vibrational modes, a two-step cooling process is required as described in the previous chapter. This process consists of cooling stages and intermittent stages. The purpose of the cooling stages is to cool a single collective phonon mode of the atoms very rapidly to very low temperatures, while the intermittent stages are needed to re-distribute energy between all the different collective vibrational modes, as illustrated in Fig. 6.1. Eventually, this process can result in the effective cooling of an atomic gas to very low temperatures. As one would expect, elastic collisions are a very effective tool to distribute energy between different collective vibrational modes of an atomic gas via thermalisation. These collisions transfer the atomic gas into its thermal state without changing the temperature of the atomic gas. In addition, their presence

effectively increases the frequency of the trapping potential. As a result, the laser cooling of a collective mode of the atoms during the cooling stage becomes even more effective than it would be in the absence of these exchange interactions.

In order to implement the proposed cooling process, we need a strongly confined atomic gas with strong elastic collisions inside an optical cavity with access to laser driving. Aljaloud *et al.* (2020), we propose to implement the experimental setup which contains all of the above components a liquid, like water, as illustrated in Fig. 6.1. The overall aim of the proposed cooling process is to lower the temperature of the liquid which surrounds , e.g. water, via sympathetic cooling. In the following we assume that there is a constant exchange thermal energy between the atomic gas and the liquid.

There are five sections in this chapter. Section 6.2 provides the experimental setup and theoretical background. In Section 6.3, we discuss the laser cooling of two indistinguishable atoms. A detailed analysis of the laser cooling of many indistinguishable particles can be found in Section 6.4. Finally, we present an overview of what is done, and summarise our findings in Section 6.5.

6.2 Experimental setup and theoretical background

In this section, we introduce the theoretical tools for the modelling of the experimental setup shown in Fig. 6.1 during the bubble collapse phase, when the bubble reaches its minimum radius. We present the relevant Hamiltonians to analyse system dynamics. The spontaneous emission of photons is, as usual, taken into account with the help of quantum optical master equations. The theoretical models which we present in this section have already been widely used to analyse the laser cooling and cavity-mediated laser cooling of single atoms.

6.2.1 Experimental setup

The experimental setup which we consider in this paper consists of a large number of strongly confined atoms. The confinement should be strong enough, so that the atoms constantly exchange vibrational energy between them. In the following

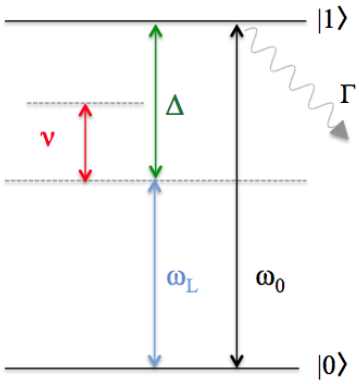

Figure 6.2: Diagrammatic representation of the level configuration of the atoms are based on ground $|0\rangle$ and excited state $|1\rangle$. Here ν and ω_{L} denote the frequency of the corresponding phonon mode and of the cooling laser. The corresponding trapping frequency of this atom is Δ. However the laser detuning $\Delta = \omega_0 - \omega_{\mathrm{L}}$. The main purpose of the laser is to excite the atom, while annihilating a phonon, If the excitation of the ion is followed by the spontaneous emission of a photon, a phonon is permanently lost, which implies cooling.

we assume that they experience strong elastic collisions. Effectively, every atom experiences a trapping potential which is due to external trapping lasers and due to the presence of the surrounding atoms. For simplicity we assume here that all atoms are essentially in the same situation and have the same phonon frequency ν. In order to cool the atoms, an external cooling laser with frequency ω_{L} is applied which pumps energy directly into the electronic states of the atoms.

Fig. 6.2 shows the relevant frequencies and detunings. As we shall see below, in order to cool the atoms, the laser frequency ω_{L} needs to be smaller than the transition frequency ω_0 between the ground state $|0\rangle$ and the excited state $|1\rangle$ of the atoms. In the following, we define the detuning Δ such that

$$\Delta \;=\; \omega_0 - \omega_{\mathrm{L}}\,. \tag{6.1}$$

In the following section, we discuss how this detuning affects the transport of phonon energy out of a cavitating bubble.

6.2.2 Interaction Hamiltonians

The total Hamiltonian of the experimental setup in Fig. 6.2 is of the form

$$H = H_{\rm atm} + H_{\rm phn} + H_{\rm int}\,, \tag{6.2}$$

as discussed in detail, for example, Blake *et al.* (2011a,b). The first two terms denote the free energy of the atoms and their vibrational modes, while the final term accounts for the laser interaction and elastic collisions between particles. Using the same notation as in the previous chapter and assuming that all atoms experience an approximately harmonic trapping potential, we find that

$$\begin{aligned} H_{\rm atm} &= \sum_{i=1}^{N} \hbar\omega_0\, \sigma_i^+\sigma_i^-\,, \\ H_{\rm phn} &= \sum_{i=1}^{N} \hbar\nu\, b_i^\dagger b_i\,. \end{aligned} \tag{6.3}$$

Here $\sigma_i^+ = |1\rangle_{ii}\langle 0|$ and $\sigma_i^- = |0\rangle_{ii}\langle 1|$ with

$$\left[\sigma_i^-, \sigma_i^+\right] = 1 - 2\sigma_i^+\sigma_i^-\,, \tag{6.4}$$

denote the raising and the lowering operator of atom i, respectively, while the operator b_i with

$$[b_i, b_i^\dagger] = 1 \tag{6.5}$$

denotes the bosonic annihilation operator of a phonon in the motion of atom i.

The applied laser field is time-dependent and hence generates a time-dependent interaction. To simplify our description of the experimental setup in Fig. 6.2 we therefore now move into the interaction picture with respect to the free Hamiltonian

$$H_0 = \sum_{i=1}^{N} \hbar\omega_{\rm L}\, \sigma_i^+\sigma_i^- \tag{6.6}$$

and take advantage of the usual rotating wave approximations. Doing so, the Hamiltonian H in Eq. (6.2) changes into the interaction Hamiltonian

$$H_{\rm I} = U_0^\dagger(t,0)\,(H - H_0)\,U_0(t,0)\,. \tag{6.7}$$

which contains the interaction term

$$U_0^\dagger(t,0)\, H_{\text{int}}\, U_0(t,0) \;=\; H_{\text{lsr}} + H_{\text{coll}}\,. \tag{6.8}$$

The first term denotes the laser interaction and the second term describes an exchange of vibrational energy due to elastic collisions.

Applying the rotating wave approximation and denoting the (real) Rabi frequency of the laser field by Ω, the laser interaction equals

$$H_{\text{lsr}} \;=\; \sum_{i=1}^{N} \frac{1}{2}\hbar\Omega \left(1 + \eta\, b_i + \eta'\, b_i^\dagger\right) \sigma_i^- + \text{H.c.} \tag{6.9}$$

to a very good approximation. This Hamiltonian simply assumes a linear coupling between atoms and phonons, while $\nu \ll \omega_0$. This is well justified, as long as η and η' are two dimensionless parameters which are much smaller than one. For example, in ion-traps this is usually the case. There $\eta = \eta'$ and both values are known as the Lamb-Dicke parameter. For simplicity, we assume that the atoms are very strongly confined thus that the distances between them are much smaller than the laser wavelength. Hence all atoms couple equally to the laser field. The first term describes atom-laser interactions without changes of vibrational states. However, the second and the third terms describe transitions which are accompanied by changes of the number of phonons in the system. In addition, collisions between the atoms are taken into account by the Hermitian Hamiltonian

$$H_{\text{coll}} \;=\; \sum_{i=1}^{N} \sum_{j\neq i} \hbar J\, b_i b_j^\dagger\,, \tag{6.10}$$

where J denotes a (real) coupling constant. Combining all of the above equations, we see that the interaction Hamiltonian H_{I} in Eq. (6.7) equals

$$\begin{aligned} H_{\text{I}} \;=\; & \sum_{i=1}^{N} \hbar\Delta\, \sigma_i^+ \sigma_i^- + \sum_{i=1}^{N} \hbar\nu\, b_i^\dagger b_i + \sum_{i=1}^{N} \sum_{j\neq i} \hbar J\, b_i b_j^\dagger \\ & + \sum_{i=1}^{N} \frac{1}{2}\hbar\Omega \left(1 + \eta\, b_i + \eta'\, b_i^\dagger\right) \sigma_i^- + \text{H.c.} \end{aligned} \tag{6.11}$$

The above ansatz assumes that all atoms experience the same interactions which is why the above Hamiltonian remains the same when exchanging two particles. Most importantly, the Hamiltonian establishes a coupling between the vibrational and the electronic states of the trapped particles.

6.2.3 Spontaneous emission from the atoms

Another important ingredient for collective laser cooling is spontaneous photon emission. Suppose all atoms couple equally to the free radiation field and are essentially indistinguishable. In the following, Γ denotes the spontaneous decay rate of a single atom in free space. Moreover, we describe our quantum system by the density matrix ρ_{I} in the interaction picture. Its dynamics is given by a master equation of Lindblad form,

$$\begin{aligned}\dot{\rho}_{\mathrm{I}} &= -\frac{\mathrm{i}}{\hbar}[H_{\mathrm{I}}, \rho_{\mathrm{I}}] \\ &\quad + \sum_{i=1}^{N}\sum_{j=1}^{N}\frac{\Gamma}{2}\left(2\sigma_i^- \rho_{\mathrm{I}} \sigma_j^+ - \sigma_i^+\sigma_j^-\rho_{\mathrm{I}} - \rho_{\mathrm{I}}\sigma_i^+\sigma_j^-\right). \end{aligned} \tag{6.12}$$

For more details of the derivation of this equation see for example(Blake *et al.* (2011a,b, 2012)).

Using density matrices, the expectation value of an observable A_{I} in the interaction picture equals $\langle A_{\mathrm{I}}\rangle_{\rho_{\mathrm{I}}} = \mathrm{Tr}(A_{\mathrm{I}}\rho_{\mathrm{I}})$. To calculate the dynamics of this expectation value, we use the master equation in Eq. (6.12) which implies that

$$\begin{aligned}\langle \dot{A}_{\mathrm{I}}\rangle &= -\frac{\mathrm{i}}{\hbar}\langle [A_{\mathrm{I}}, H_{\mathrm{I}}]\rangle \\ &\quad + \sum_{i=1}^{N}\sum_{j=1}^{N}\frac{\Gamma}{2}\left\langle 2\sigma_j^+ A_{\mathrm{I}}\sigma_i^- - A_{\mathrm{I}}\sigma_i^+\sigma_j^- - \sigma_i^+\sigma_j^- A_{\mathrm{I}}\right\rangle \end{aligned} \tag{6.13}$$

in the interaction picture. Like the interaction Hamiltonian in Eq. (6.11), both equations (6.12) and (6.13) remain invariant under particle exchange.

6.3 Laser cooling of two indistinguishable atoms

Before we introduce the collective dynamics of a laser-driven atomic gas inside a cavitating bubble, we now study the dynamics of only two atoms. Although this case might not be of any practical interest, it is simple enough for analytical calculations. It also provides crucial insight into the cooling mechanism which we consider in Section 6.4, where we use the calculations in this section to justify approximations. For example, a closer look at the interaction Hamiltonian in Eq. (6.11) and the master equations in Eq. (6.12) shows that both equations are completely symmetric with respect to exchanging particles. In principle, we should be able to use this observation to simplify calculations. However, this applies only to a certain extent. As we shall see below, symmetric atomic states couple to anti-symmetric atomic states, since the overall symmetry of the atom-phonon system can be preserved by simultaneously coupling symmetric to anti-symmetric phonon states. This complicates the dynamics of the system which we consider here.

6.3.1 Basic idea

Nevertheless, it is advantageous to change notation and to introduce collective operators which are either symmetric or anti-symmetric with respect to an exchange of atom 1 and 2. For example, in the following we consider the collective phonon annihilation operators $b_\pm$ with

$$b_\pm \;=\; (b_1 \pm b_2)/\sqrt{2}\,. \tag{6.14}$$

Like b_1 and b_2, they obey bosonic commutator relations,

$$[b_\pm, b_\pm^\dagger] = 1\,, \quad [b_\pm, b_\pm] = [b_\pm, b_\mp^\dagger] = 0\,. \tag{6.15}$$

In addition, we introduce a complete set of symmetric and antisymmetric atomic basis states,

$$\begin{aligned} |g\rangle &= |00\rangle\,, \quad |s\rangle = (|01\rangle + |10\rangle)/\sqrt{2}\,, \\ |a\rangle &= (|01\rangle - |10\rangle)/\sqrt{2}\,, \quad |e\rangle = |11\rangle\,, \end{aligned} \tag{6.16}$$

and atomic lowering and raising operators such that

$$\begin{aligned} \sigma_{xy} &= |x\rangle\langle y|\,, \\ \sigma_+^- &= \sigma_{gs} + \sigma_{se}\,, \\ \sigma_-^- &= -\sigma_{ga} + \sigma_{ae}\,. \end{aligned} \tag{6.17}$$

Using this notation, the interaction Hamiltonian in Eq. (6.11) can be shown to equal

$$\begin{aligned} H_{\mathrm{I}} &= \hbar\Delta\left(\sigma_+^+\sigma_+^- + \sigma_-^+\sigma_-^-\right) \\ &\quad +\hbar(\nu+J)\,b_+^\dagger b_+ + \hbar(\nu-J)\,b_-^\dagger b_- \\ &\quad +\frac{1}{2}\hbar\Omega\left(\sqrt{2} + \eta\,b_+ + \eta'\,b_+^\dagger\right)\sigma_+^- + \mathrm{H.c.} \\ &\quad +\frac{1}{2}\hbar\Omega\left(\eta\,b_- + \eta'\,b_-^\dagger\right)\sigma_-^- + \mathrm{H.c.} \end{aligned} \tag{6.18}$$

Moreover, Eq. (6.13) which describes the dynamics of expectation values simplifies to

$$\begin{aligned} \langle \dot{A}_{\mathrm{I}}\rangle &= -\frac{\mathrm{i}}{\hbar}\langle[A_{\mathrm{I}}, H_{\mathrm{I}}]\rangle \\ &\quad +\Gamma\langle 2\,\sigma_+^+ A_{\mathrm{I}}\sigma_+^- - A_{\mathrm{I}}\sigma_+^+\sigma_+^- - \sigma_+^+\sigma_+^- A_{\mathrm{I}}\rangle \end{aligned} \tag{6.19}$$

for $N = 2$. The spontaneous decay rate of the excited symmetric states $|s\rangle$ and $|e\rangle$ is collectively enhanced. It equals 2Γ which is twice the spontaneous decay rate of a single atom. In contrast to this, the anti-symmetric state $|a\rangle$ of the atoms does not emit photons.

In the following, we are especially interested in how the total mean number of phonons m of the two atoms evolves in time. One can easily check that this number is the sum of the mean phonon numbers of the b_+ and the b_- phonon mode, i.e.

$$m = m^{(+)} + m^{(-)} \tag{6.20}$$

with $m^{(\pm)} = \langle b_\pm^\dagger b_\pm\rangle$. Although the interaction Hamiltonian H_{I} in Eq. (6.18) does not seem to contain any interactions between $+$ and $-$ operators, we cannot analyse the dynamics of $m^{(-)}$ and $m^{(+)}$ separately. The reason for this is that the $\sigma_\pm^-$ operators in Eq. (6.17) both involve the atomic states $|g\rangle$ and $|e\rangle$.

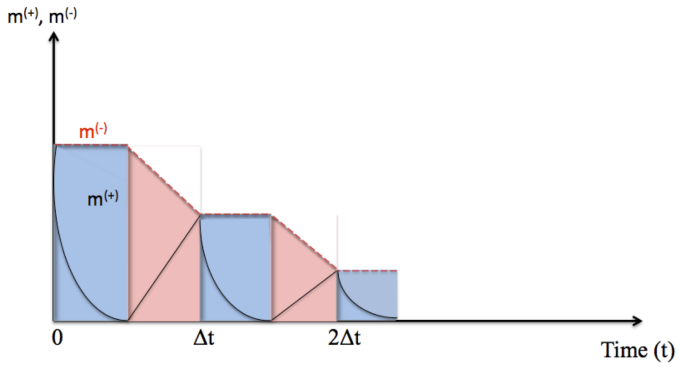

Figure 6.3: Schematic view of the expected dynamics of $m^{(+)}$ and $m^{(-)}$ during alternating cooling (blue) and thermalisation stages(pink). During cooling stages, $m^{(+)}$ drops rapidly and becomes very small. The main purpose of the intermittent thermalisation stages is to transfer energy from the b_- into the now empty b_+ phonon mode. Both phonon modes lose their energy and the two atoms become eventually very cold.

However, as we shall see below, it is nevertheless advantageous to use the above notation. In the following subsection, it is shown that the cooling laser only reduces the mean number of phonons in the b_+ mode, while the mean number of phonons in the b_- mode remains essentially the same during cooling stages. This is illustrated in Fig. 6.3 which sketches the dynamics of $m^{(+)}$ and $m^{(-)}$ during alternating cooling and thermalisation stages. During cooling stages, $m^{(+)}$ drops rapidly and becomes very small. The main purpose of the intermittent thermalisation stages is to transfer energy from the b_- into the now empty b_+ phonon mode. In this way, both phonon modes lose their energy and the two atoms become eventually very cold.

Fig. 6.4(a) shows all atomic transitions which participate in the cooling process of the b_+ mode. As we shall see below, cooling only occurs on a time scale given by the cooling rate

$$\gamma_{\text{cool}} = \frac{(\eta'\Omega)^2}{2\Gamma}. \tag{6.21}$$

As usual, the cooling process is relatively slow. Our calculations in the next subsection also show that only the atomic states $|g\rangle$ and $|s\rangle$ participate actively

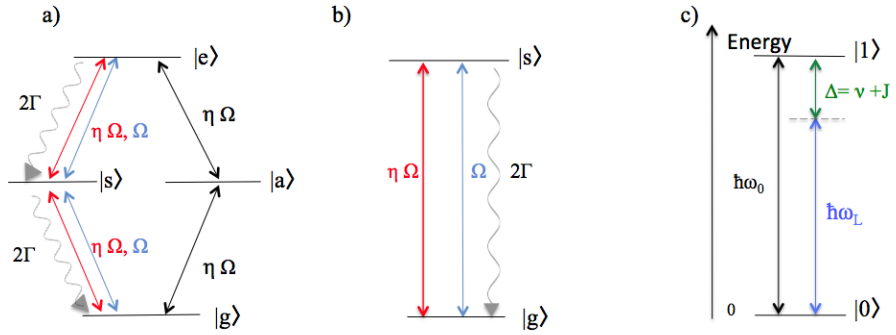

Figure 6.4: Diagrammatic representation of the level configuration of the atoms are based on ground $|g\rangle$ and first excited state $|s\rangle$. Here ν and ω_{L} denote the frequency of the corresponding phonon mode and of the cooling laser. The corresponding trapping frequency of this atom is Δ. However the laser detuning $\Delta = \omega_0 - \omega_{\mathrm{L}}$. The main purpose of the laser is to excite the atom, while annihilating a phonon, If the excitation of the ion is followed by the spontaneous emission of a photon, a phonon is permanently lost, which implies cooling. (b) In the cooling process, only the atomic states $|g\rangle$ and $|s\rangle$ actively participate. (c) The laser detuning Δ of the cooling laser from the 0 -1 transition of the atoms equals $\nu + J$.

in the cooling process of the b_+ mode (cf. Fig. 6.4(b)). Any population in the two remaining atomic states, $|a\rangle$ and $|e\rangle$, is essentially negligible. This means, the cooling phase of laser cooling of two indistinguishable particles inside a cavitating bubble has many similarities with the laser cooling of a single trapped particle (Blake *et al.* (2011b)). As illustrated in Fig. 6.4(b), this equivalent particle would have a ground state $|g\rangle$ and an excited state $|s\rangle$. Its spontaneous decay rate would have to be twice the decay rate of a single atom, i.e. 2Γ, but its laser coupling constant $\eta'\Omega$ would be the same Blake *et al.* (2011b). The cooling process of the b_+ phonon mode is therefore *not* collectively enhanced, as one might naively expect. To avoid the above described reduction of the cooling rate compared to the laser cooling rate of a single trapped atom, the atomic gas needs to be placed into an opaque cavitating bubble where the relevant spontaneous decay rate does not depend on the number of atoms inside the gas (Aljaloud *et al.* (2020)).

The most efficient laser cooling of the two atoms occurs during the bubble collapse phase when the phonon frequency ν and the atom collision rate J assume their maximum values, ν_0 and J_0. In order to maximise the cooling process, we therefore propose to choose the laser detuning Δ of the cooling laser from the 0-1 transition of the atoms equals $\nu + J$ at this point,

$$\Delta \;=\; \nu_0 + J_0\,, \tag{6.22}$$

at least to a very good approximation. As one can see from Eq. (6.18), in the presence of collisions, $\hbar(\nu_0 + J_0)$ equals the energy of a single phonon in the b_+ phonon mode during the cooling phase. The above comparison with the laser cooling of a single atom therefore suggests to choose Δ as in Eq. (6.22) and as illustrated in Fig. 6.4(c). Moreover, efficient laser cooling requires that the laser detuning Δ is much larger than the laser Rabi frequency,

$$\Omega \;\ll\; \Gamma \;\ll\; \Delta\,. \tag{6.23}$$

In this case, the transfer of the atoms from $|g\rangle$ to $|s\rangle$ is most likely accompanied by the annihilation of a b_+ phonon. All other excitation processes are strongly detuned. When the atoms subsequently return from $|s\rangle$ to $|g\rangle$ via the spontaneous emission of a photon, this phonon is permanently lost. The mean number of phonons in the system has been reduced by one which implies cooling. When the cavitating bubble does not experience a collapse phase, the phonon frequency ν and the collision rate J are too small for any atomic dynamics to occur which is why efficient cooling only takes place during the bubble collapse phase. Even if we would reduce the laser detuning to keep cooling processes on resonance, the cooling would become less efficient, since also condition (6.23) must be met.

Finally, let us assume that the cooling laser reduces the mean number in the b_+ phonon mode very effectively and $m^{(+)}$ is efficiently zero at the end of the cooling phase. To complete a single cooling cycle, the cooling phase is followed by a thermalisation phase, as illustrated in Fig. 6.3. During each thermalisation stage, both atoms eventually reach their thermal state which then adiabatically changes as the phonon frequency ν and the collision rate J change in time. For example, if collisions between the atoms are negligible, then $J = 0$ and $m^{(+)} = m^{(-)}$ at the end of each thermalisation stage. This means, each cooling cycle halves the total

phonon number. Hence, after M repetitions of cooling and themalisation stages, we have

$$m^{(+)}(M\Delta t) \;=\; \frac{1}{2^M}\, m^{(+)}(0)\,. \tag{6.24}$$

This means, the thermal energy of the atoms drops very rapidly. As we shall see below, the same applies for $J_0 \neq 0$. If the common b_+ phonon mode can be cooled very efficiently, then both atoms should eventually end up at a very low temperature.

6.3.2 Cooling stages

Next we analyse the dynamics of $m^{(-)}$ and $m^{(+)}$ during the bubble collapse phase, when the conditions in Eqs. (6.22) and (6.23) apply. In order to get a closed set of rate equations, we now describe the dynamics the expectation values of the general form

$$\begin{aligned} d_{xy}^{(\pm)} &= \mathrm{i}\,\langle b_\pm \sigma_{xy} - b_\pm^\dagger \sigma_{yx}\rangle\,, \\ f_{xy}^{(\pm)} &= \langle b_\pm \sigma_{xy} + b_\pm^\dagger \sigma_{yx}\rangle \end{aligned} \tag{6.25}$$

with $x, y = a, s, e$. All of the above expectation values are real. Taking the results of the previous subsection into account and substituting the interaction Hamiltonian H_I in Eq. (6.18) into Eq. (6.19), one can show that

$$\begin{aligned} \dot{m}^{(+)} &= \frac{1}{2}\eta\Omega\,[d_{gs}^{(+)} + d_{se}^{(+)}] + \frac{1}{2}\eta'\Omega\,[d_{sg}^{(+)} + d_{es}^{(+)}]\,, \\ \dot{m}^{(-)} &= -\frac{1}{2}\eta\Omega\,[d_{ga}^{(-)} - d_{ae}^{(-)}] - \frac{1}{2}\eta'\Omega\,[d_{ag}^{(-)} - d_{ea}^{(-)}]\,. \end{aligned} \tag{6.26}$$

In the remainder of this subsection, we calculate the expectation values on the right hand side of this equation in zeroth order in η and η'.

1. Time evolution of $m^{(-)}$ in first order in η and η'

First let us describe the dynamics of the $m^{(-)}$ phonons. Substituting the interaction Hamiltonian H_I in Eq. (6.18) again into Eq. (6.19), while assuming that

$\eta = \eta' = 0$, we now obtain two sets of independent linear differential equations. More concretely, we find that

$$\begin{aligned}
\dot{d}_{ga}^{(-)} &= (\Delta + \nu_0 - J_0) f_{ga}^{(-)} - \tilde{\Omega}\, f_{sa}^{(-)}\,, \\
\dot{f}_{ga}^{(-)} &= -(\Delta + \nu_0 - J_0) d_{ga}^{(-)} + \tilde{\Omega}\, d_{sa}^{(-)}\,, \\
\dot{d}_{ea}^{(-)} &= -(\Delta - \nu_0 + J_0) f_{ea}^{(-)} - \tilde{\Omega}\, f_{sa}^{(-)} - \Gamma\, d_{ea}^{(-)}\,, \\
\dot{f}_{ea}^{(-)} &= (\Delta - \nu_0 + J_0) d_{ea}^{(-)} + \tilde{\Omega}\, d_{sa}^{(-)} - \Gamma\, f_{ea}^{(-)}\,, \\
\dot{d}_{sa}^{(-)} &= (\nu_0 - J_0) f_{sa}^{(-)} - \tilde{\Omega}[f_{ga}^{(-)} + f_{ea}^{(-)}] - \Gamma\, d_{sa}^{(-)}\,, \\
\dot{f}_{sa}^{(-)} &= -(\nu_0 - J_0) d_{sa}^{(-)} + \tilde{\Omega}[d_{ga}^{(-)} + d_{ea}^{(-)}] - \Gamma\, f_{sa}^{(-)}\,.
\end{aligned} \tag{6.27}$$

In addition, one can show that

$$\begin{aligned}
\dot{d}_{ag}^{(-)} &= -(\Delta - \nu_0 + J_0) f_{ag}^{(-)} + \tilde{\Omega}\, f_{as}^{(-)}\,, \\
\dot{f}_{ag}^{(-)} &= (\Delta - \nu_0 + J_0) d_{ag}^{(-)} - \tilde{\Omega}\, d_{as}^{(-)}\,, \\
\dot{d}_{ae}^{(-)} &= (\Delta + \nu_0 - J_0) f_{ae}^{(-)} + \tilde{\Omega}\, f_{as}^{(-)} - \Gamma\, d_{ae}^{(-)}\,, \\
\dot{f}_{ae}^{(-)} &= -(\Delta + \nu_0 - J_0) d_{ae}^{(-)} - \tilde{\Omega}\, d_{as}^{(-)} - \Gamma\, f_{ae}^{(-)}\,, \\
\dot{d}_{as}^{(-)} &= (\nu_0 - J_0) f_{as}^{(-)} + \tilde{\Omega}[f_{ag}^{(-)} + f_{ae}^{(-)}] - \Gamma\, d_{as}^{(-)}\,, \\
\dot{f}_{as}^{(-)} &= -(\nu_0 - J_0) d_{as}^{(-)} - \tilde{\Omega}[d_{ag}^{(-)} + d_{ae}^{(-)}] - \Gamma\, f_{as}^{(-)}\,.
\end{aligned} \tag{6.28}$$

Here the laser Rabi frequency $\tilde{\Omega}$ is defined such that

$$\tilde{\Omega} \;=\; \Omega/\sqrt{2}\,. \tag{6.29}$$

Suppose the two atoms do not experience any laser driving between cooling stages. Hence, their state is given by the ground state $|g\rangle$ at the beginning of every cooling state. As a result, all of the expectation values on the right hand side of Eqs. (6.27) and (6.28) are initially equal to zero,

$$d_{xy}^{(-)} = f_{xy}^{(-)} \;=\; 0\,, \tag{6.30}$$

where $x, y = g, s, a, e$. Since the above equations are linear differential equations without any constant terms, Eq. (6.30) remains valid throughout the whole cooling process. Eq. (6.26) therefore shows that

$$\dot{m}^{(-)} \;=\; 0 \tag{6.31}$$

in first order in η and η'. If the b_- phonon mode experiences cooling or heating, this cooling or heating only occurs on a relatively slow time scale. Their cooling rates are at least of second order in η and η'. To a very good approximation, m_- remains the constant during cooling stages.

2. Time evolution of $m^{(+)}$ in first order in η and η'

Next we describe the dynamics of the b_+ phonon mode. Proceeding as above and deriving rate equations for the $d_{xy}^{(+)}$ and the $f_{xy}^{(+)}$ variables, we find that

$$\begin{aligned}
\dot{d}_{sg}^{(+)} &= -(\Delta-\nu_0-J_0)f_{sg}^{(+)} - \tilde{\Omega}[f_{eg}^{(+)}+f_{gg}^{(+)}-f_{ss}^{(+)}] \\
&\quad -\Gamma[d_{sg}^{(+)}-2d_{es}^{(+)}]\,, \\
\dot{f}_{sg}^{(+)} &= (\Delta-\nu_0-J_0)d_{sg}^{(+)} + \tilde{\Omega}[d_{eg}^{(+)}+d_{gg}^{(+)}-d_{ss}^{(+)}] \\
&\quad -\Gamma[f_{sg}^{(+)}-2f_{es}^{(+)}]\,, \\
\dot{d}_{es}^{(+)} &= -(\Delta-\nu_0-J_0)f_{es}^{(+)} + \tilde{\Omega}[f_{eg}^{(+)}-f_{ss}^{(+)}+f_{ee}^{(+)}] \\
&\quad -2\Gamma\, d_{es}^{(+)}\,, \\
\dot{f}_{es}^{(+)} &= (\Delta-\nu_0-J_0)d_{es}^{(+)} - \tilde{\Omega}[d_{eg}^{(+)}-d_{ss}^{(+)}+d_{ee}^{(+)}] \\
&\quad -2\Gamma\, f_{es}^{(+)}
\end{aligned} \tag{6.32}$$

for $\eta=\eta'=0$. In addition, one can show that

$$\begin{aligned}
\dot{d}_{gs}^{(+)} &= (\Delta+\nu_0+J_0)f_{gs}^{(+)} + \tilde{\Omega}[f_{ge}^{(+)}+f_{gg}^{(+)}-f_{ss}^{(+)}] \\
&\quad -\Gamma[d_{gs}^{(+)}-2d_{se}^{(+)}]\,, \\
\dot{f}_{gs}^{(+)} &= -(\Delta+\nu_0+J_0)d_{gs}^{(+)} - \tilde{\Omega}[d_{ge}^{(+)}-d_{gg}^{(+)}+d_{ss}^{(+)}] \\
&\quad -\Gamma[f_{gs}^{(+)}-2f_{se}^{(+)}]\,, \\
\dot{d}_{se}^{(+)} &= (\Delta+\nu_0+J_0)f_{se}^{(+)} - \tilde{\Omega}[f_{ge}^{(+)}-f_{ss}^{(+)}+f_{ee}^{(+)}] \\
&\quad -2\Gamma\, d_{se}^{(+)}\,, \\
\dot{f}_{se}^{(+)} &= -(\Delta+\nu_0+J_0)d_{se}^{(+)} + \tilde{\Omega}[d_{ge}^{(+)}-d_{ss}^{(+)}+d_{ee}^{(+)}] \\
&\quad -2\Gamma\, f_{se}^{(+)}\,.
\end{aligned} \tag{6.33}$$

Moreover, proceeding as above, we obtain the differential equations

$$\dot{d}_{ge}^{(+)} = (2\Delta+\nu_0+J_0)f_{ge}^{(+)} + \tilde{\Omega}[f_{gs}^{(+)}-f_{se}^{(+)}] - \Gamma\, d_{ge}^{(+)}\,,$$

$$
\begin{aligned}
\dot{f}_{ge}^{(+)} &= -(2\Delta+\nu_0+J_0)d_{ge}^{(+)} - \tilde{\Omega}[d_{gs}^{(+)} - d_{se}^{(+)}] - \Gamma\, f_{ge}^{(+)}\,, \\
\dot{d}_{eg}^{(+)} &= -(2\Delta-\nu_0-J_0)f_{eg}^{(+)} - \tilde{\Omega}[f_{sg}^{(+)} - f_{es}^{(+)}] - \Gamma\, d_{eg}^{(+)}\,, \\
\dot{f}_{eg}^{(+)} &= (2\Delta-\nu_0-J_0)d_{eg}^{(+)} + \tilde{\Omega}[d_{sg}^{(+)} - d_{es}^{(+)}] - \Gamma\, f_{eg}^{(+)}\,,
\end{aligned} \tag{6.34}
$$

while

$$
\begin{aligned}
\dot{d}_{gg}^{(+)} &= (\nu_0+J_0)f_{gg}^{(+)} + \tilde{\Omega}[f_{gs}^{(+)} - f_{sg}^{(+)}] + 2\Gamma\, d_{ss}^{(+)}\,, \\
\dot{f}_{gg}^{(+)} &= -(\nu_0+J_0)d_{gg}^{(+)} - \tilde{\Omega}[d_{gs}^{(+)} - d_{sg}^{(+)}] + 2\Gamma\, f_{ss}^{(+)}\,, \\
\dot{d}_{ss}^{(+)} &= (\nu_0+J_0)f_{ss}^{(+)} - \tilde{\Omega}[f_{gs}^{(+)} - f_{sg}^{(+)} - f_{se}^{(+)} + f_{es}^{(+)}] \\
&\quad -2\Gamma[d_{ss}^{(+)} - d_{ee}^{(+)}]\,, \\
\dot{f}_{ss}^{(+)} &= -(\nu_0+J_0)d_{ss}^{(+)} + \tilde{\Omega}[d_{gs}^{(+)} - d_{sg}^{(+)} - d_{se}^{(+)} + d_{es}^{(+)}] \\
&\quad -2\Gamma[f_{ss}^{(+)} - f_{ee}^{(+)}]\,, \\
\dot{d}_{ee}^{(+)} &= (\nu_0+J_0)f_{ee}^{(+)} - \tilde{\Omega}[f_{se}^{(+)} - f_{es}^{(+)}] - 2\Gamma\, d_{ee}^{(+)} \\
\dot{f}_{ee}^{(+)} &= -(\nu_0+J_0)d_{ee}^{(+)} + \tilde{\Omega}[d_{se}^{(+)} - d_{es}^{(+)}] - 2\Gamma\, f_{ee}^{(+)}
\end{aligned} \tag{6.35}
$$

in zeroth order in η and η'. One can easily check that Eqs. (6.32)-(6.35) form a closed set of differential equations which can be solved, at least in principle, numerically and analytically.

When the cooling laser is turned off, the atoms might emit one or two more photons but eventually they return into their ground state $|g\rangle$. In following, we therefore assume that all expectation values with $d_{xy}^{(+)}$ and $f_{xy}^{(+)}$ and initially zero, with $x = y = g$ being the only exception. However, $d_{gg}^{(+)}$ and $f_{gg}^{(+)}$ denote the average momentum and the average position of the two atoms inside the trap. Since the atoms are trapped and as long as the trap is symmetric around its center at $x = 0$, both variables are zero in the thermal state which implies that

$$
d_{gg}^{(+)} = f_{gg}^{(+)} \;=\; 0\,, \tag{6.36}
$$

at the beginning of every cooling phase (see next subsection for more details). Hence the variables on the right hand side of Eq. (6.26) remain zero once the cooling laser is turned on and the mean number of phonons in the b_+ mode remains the same.

3. Time evolution of $m^{(+)}$ in second order in η and η'

To describe the expected cooling process we need to go a step further and terms of the order η and η' need to be taken into account, if we want to derive effective cooling rates. Even in zeroth order in η and η', the above equations are hard to solve analytically. However, in the following, we are especially interested in the parameter regime where Eqs. (6.22) and (6.23) apply. In this case, the dynamics of all the variables in Eqs. (6.33) to (6.35) are strongly detuned. In the following, we therefore assume that the variables in the indices gs, se, ge, eg, ss and ee remain zero throughout the cooling process. Making this approximation, Eq. (6.32) simplifies to

$$\begin{aligned} \dot{d}_{sg}^{(+)} &= -\Gamma\, d_{sg}^{(+)} + 2\Gamma\, d_{es}^{(+)}\,, \\ \dot{f}_{sg}^{(+)} &= -\Gamma\, f_{sg}^{(+)} + 2\Gamma\, f_{es}^{(+)}\,, \\ \dot{d}_{es}^{(+)} &= -2\Gamma\, d_{es}^{(+)}\,, \\ \dot{f}_{es}^{(+)} &= -2\Gamma\, f_{es}^{(+)}\,. \end{aligned} \tag{6.37}$$

Moreover, taking terms in first order in η and η' into account and neglecting again any variables with indices gs, se, ge, eg, ss and ee, we see that

$$\begin{aligned} \dot{d}_{sg}^{(+)} &= -\frac{1}{2}\Omega\,[\eta\, l_{gg}^{(+)} + 2\eta' q_{gg}^{(+)}] - \Gamma\, d_{sg}^{(+)} + 2\Gamma\, d_{es}^{(+)}\,, \\ \dot{f}_{sg}^{(+)} &= \frac{1}{2}\eta\Omega\, h_{gg}^{(+)} - \Gamma\, f_{sg}^{(+)} + 2\Gamma\, f_{es}^{(+)}\,, \\ \dot{d}_{es}^{(+)} &= -2\Gamma\, d_{es}^{(+)}\,, \\ \dot{f}_{es}^{(+)} &= -2\Gamma\, f_{es}^{(+)}\,, \end{aligned} \tag{6.38}$$

where we defined

$$\begin{aligned} l_{xx}^{(+)} &= \langle (b_+^2 + b_+^{\dagger 2})\sigma_{xx}\rangle\,, \\ h_{xx}^{(+)} &= \mathrm{i}\,\langle (b_+^2 - b_+^{\dagger 2})\sigma_{xx}\rangle\,, \\ q_{xx}^{(+)} &= \langle b_+^\dagger b_+ \sigma_{xx}\rangle\,. \end{aligned} \tag{6.39}$$

In zeroth order in η and η', we find that $l_{gg}^{(+)}$ evolves rapidly on the time scale given by $\nu_0 + J_0$. Moreover, the above calculations suggest that the two atoms remain predominantly in their ground state $|g\rangle$. This suggests that

$$l_{gg}^{(+)} = 0 \quad \text{and} \quad q_{gg}^{(+)} = m^{(+)}\,. \tag{6.40}$$

Adiabatically eliminating $d_{sg}^{(+)}$ and $f_{es}^{(+)}$ from the system dynamics by setting their time derivatives in Eq. (6.38) equal to zero therefore yields

$$d_{sg}^{(+)} = -\frac{\eta'\Omega}{\Gamma} m^{(+)} . \tag{6.41}$$

The reason for this is that the above equations describe rapid damped oscillations which result relatively quickly in a stationary state. While most variables remain zero in first order in η and η', the coherence $d_{sg}^{(+)}$ assumes a value which is non-zero.

Substituting the result in Eq. (6.41) into Eqs. (6.26), we finally obtain the cooling equation

$$\dot{m}^{(+)} = -\gamma_{\text{cool}} m^{(+)} \tag{6.42}$$

with the (positive) cooling rate to a very good approximation given by γ_{cool} in Eq. (6.21). Eq. (6.42) can now be solved relatively easily. The standard solution to this differential equation is of course

$$\dot{m}^{(+)}(t) = \mathrm{e}^{-\gamma_{\text{cool}} t} m^{(+)}(0) . \tag{6.43}$$

The mean number of phonons in the b_+ mode decreases exponentially. Given the cooling stage is sufficiently long, all phonons are converted into atomic excitations and leave the system via spontaneous photon emission, as described in Section 6.3.1.

In laser cooling of trapped ions, the minimum phonon number that can be achieved during cooling stages is indeed very low. Trapped ions are routinely cooled down to nanokelvin temperature . The only requirements for this to work is that the phonon frequency ν_0 of the trapped atomic particles is sufficiently large when compared to the relevant spontaneous decay rate Γ. Without restrictions we assume here that the conditions for cooling to very low temperatures hold. Being a solid state and not a quantum optical system, we expect phonon frequencies ν_0 to be much larger than in ion trap experiments, while the order of magnitude of the spontaneous decay rate Γ of the trapped atoms should be about the same. For more details, see Ref. Aljaloud *et al.* (2020)

The main problems of laser cooling indistinguishable particles inside cavitating bubbles are different in nature. While the parameter regimes which allow

reaching very low temperatures might be more readily available than in ion trap experiments, cooling stages might be relatively short. Once the collapse phase comes to an end and the bubble radius increases again, the phonon number ν decreases rapidly and the collisions between the atoms with rate J disappear. The cooling laser is therefore no longer in resonance with the above described cooling processes and the cooling disappears until the next collapse phase. Moreover, the cooling laser only reduces the mean number of phonons in the b_+ mode. To remove all phonons from the system, another mechanisms is needed which transfers vibrational energy from the b_- into the b_+ mode between cooling stages.

6.3.3 Thermalisation stages

As mentioned already earlier, this is exactly the purpose of the thermalisation stages. Once the bubble radius increases again, the phonon frequency ν and the collision rate J of the atoms decreases significantly and the atoms no longer experience the cooling laser. Instead they evolve according to the laws of thermodynamics and adiabatically exchange vibrational energy with each other and their environment. For simplicity we ignore any heat exchange with the surrounding liquid in the following. In this case, the atoms assume thermal states which change as their phonon frequencies and collisions rates change in time. Since we are especially interested in the state of the atoms at the beginning of the next cooling stage, we can assume that their Hamiltonian equals

$$H_{\mathrm{I}} \;=\; \hbar(\nu_0 + J_0)\, b_+^\dagger b_+ + \hbar(\nu_0 - J_0)\, b_-^\dagger b_- \tag{6.44}$$

which is the Hamiltonian H_{I} in Eq. (6.18) but with the laser Rabi frequency still effectively equal to zero ($\Omega = 0$). Moreover, we ignore the electronic states of the atoms. For atomic transition frequencies ω_0 in the optical regime, the thermal state of the atoms is to a very good approximation the same as the ground state $|g\rangle$. From Eq. (6.44) we see that we are effectively looking for the thermal state of two non-interacting harmonic oscillators whose total energy is the same as the vibrational energy at the end of the previous cooling stage.

The thermal state of two harmonic oscillators

Here we are especially interested in the thermal state of two atoms with elastic collisions with their interaction Hamiltonian H_{I} given in Eq. (6.44). During thermalisation stages, the phonon frequency ν and the collision rate J are still relatively small and the applied cooling laser field is therefore in general strongly detuned. This is why we can neglect any additional terms in the above equation and only need to consider the phonon states of the system, while assuming that the atoms remain in their common ground state $|g\rangle$. Unfortunately, the above Hamiltonian automatically results in a thermal state with $d_{gg}^{(+)}$ and $f_{gg}^{(+)}$ both equal to zero, as we assumed in Eq. (6.36) the previous subsection for a symmetric trapping potential. Using Eq. (3.33), one can show that

$$m^{(\pm)} = \frac{\mathrm{e}^{-\lambda^{(\pm)}}}{\mathrm{e}^{-\lambda^{(\pm)}} - 1}, \tag{6.45}$$

where, the parameter $\lambda = \beta\hbar\omega$,

$$\lambda^{(\pm)} = \beta\hbar(\nu_0 \pm J_0) \tag{6.46}$$

and where β is defined as $\beta = \frac{1}{k_{\mathrm{B}}T}$. The temperature T of the two atoms at the end of the thermalisation stage depends on their phonon energy at the end of the previous cooling stage. During thermalisation, the phonon energy of the two atoms remains the same.

6.3.4 Final phonon numbers of a two-step laser cooling process

Suppose we alternate cooling states and thermalisation stages as shown in Fig. 6.3. As we have seen in the previous subsection, each thermalisation stage results in a transfer of some of the vibrational energy of the b_- phonon mode of the atoms into the b_+ mode. As described in Section 6.3.2, this phonon mode is subsequently emptied during a cooling stage. For simplicity, and also since it applies to a very

good approximation, we assume in the following that the cooling stage is long enough to cool the $b^{(+)}$ mode until

$$m^{(+)} \;=\; 0 \tag{6.47}$$

and neglect any possible heating transitions. As we have seen in Section 6.3.2, the latter assumption is well justified. Eventually, this process will remove all energy from all vibrational modes of the two atoms. This is illustrated in Fig. 6.3. In this subsection, we now introducet how the temperature of the atoms changes after M cooling and thermalisation stages.

Suppose $m^{(+)}(0)$ is the mean number of phonons in the b_+ phonon mode at the beginning of the first cooling phase at $t = 0$. Using the equations in the previous sections, we now calculate how this number changes from one cooling cycle to the beginning of the next. Of course, the experimental parameters ν and J change a lot during thermalisation stages. However, here we are especially interested in their maximum values ν_0 and J which they assume during the bubble collapse phase. In addition, we assume in the following that the absorption of energy from the liquid surrounding the bubble remains negligible throughout the cooling process. Taking this into account as well as the fact that the b_+ mode is depleted during the cooling stage, energy conservation implies that

$$\begin{aligned} \hbar(\nu_0 - J)\, m^{(-)}(0) \;&=\; \hbar(\nu_0 + J)\, m^{(+)}(\Delta t) \\ &\quad +\hbar(\nu_0 - J)\, m^{(-)}(\Delta t)\,, \end{aligned} \tag{6.48}$$

where Δt denotes the duration of a single cooling cycle. From Eq. (6.46), we see that $\lambda^{(+)}(\Delta t) = A\lambda^{(-)}(\Delta t)$ with

$$A \;=\; \frac{\nu_0 - J}{\nu_0 + J}\,. \tag{6.49}$$

Combining Eqs. (6.45) and (6.46) with Eq. (6.49) and calculating $m^{(+)}(\Delta t)$ as a function of $m^{(-)}(\Delta t)$, we hence find that

$$m^{(+)}(\Delta t) \;=\; \frac{m^{(-)}(\Delta t)^A}{m^{(-)}(\Delta t)^A - [m^{(-)}(\Delta t) - 1]^A}\,. \tag{6.50}$$

In principle, the above equations can be used to calculate how $m^{(-)}(\Delta t)$ depends on $m^{(-)}(0)$ which tells us, how the mean number of phonons in the b_- mode

changes from one cycle of the cooling process to the next. Unfortunately, solving the above equations is not straightforward, which is why we first describe the simple case where $A = 1$.

In the absence of any collisions, we have $J = 0$. In this case, $A = 1$ and $m^{(+)}(\Delta t) = m^{(-)}(\Delta t)$. Hence, Eq. (6.48) shows that the mean number of phonons in the b_- modes is halved in every cooling cycle. After M repetitions, the mean number of phonons in the b_- mode which is the same as the mean number of phonons in the b_+ mode therefore equals $m^{(-)}(M\Delta t)$ in Eq. (6.24). Under ideal cooling conditions, there is thus nothing which stops the phonon modes from emptying and eventually $m^{(+)}$ and $m^{(-)}$ reduce to zero. This means, the final temperature of the atoms can be very close to zero. The only restrictions come from highly-detuned off-resonant heating transitions which we neglected when we analysed the cooling dynamics of the two atoms in Section 6.3.2.

In general, for $J \neq 0$, the cooling cycle stops and no longer reduces the mean phonon number in the b_- mode when $m^{(-)}(0)$ becomes so small that

$$m^{(-)}(\Delta t) \;=\; m^{(-)}(0)\,. \tag{6.51}$$

Substituting this relation into Eq. (6.48), we immediately see that this condition only applies once

$$m^{(-)} \;=\; 0 \tag{6.52}$$

which is the stationary point of the above equation. For $m^{(-)}(0) = 0$, we automatically have $m^{(-)}(\Delta t) = 0$. Under ideal cooling conditions, there is thus nothing which stops the phonon modes from emptying and eventually $m^{(+)}$ and $m^{(-)}$ reduce to zero.

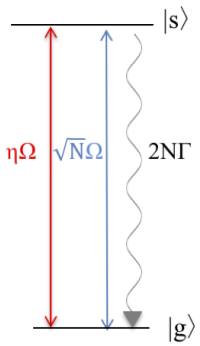

Figure 6.5: Diagrammatic representation of the level configuration of the atoms are based on ground $|g\rangle$ and first excited state $|s\rangle$.

6.4 Laser cooling of many indistinguishable particles

In the previous Section, we have seen that the cooling dynamics of two indistinguishable atomic particles is equivalent to the cooling dynamics of a single atom. Even in the presence of additional atomic states, only the ground state and a single excited state contribute to the cooling dynamics of the system on the relatively fast time scale given by the cooling rate γ_{cool} in Eq. (6.21). The presence of any other atomic states, even when they experience the cooling laser, can be ignored. In the following this is taken into account when analysing the cooling dynamics of many indistinguishable atomic particles inside a cavitating bubble. The experimental setup with many atoms is very similar to the setup which we described in pervious section and has already been introduced in Section 6.2, as illustrated in Fig. 6.5. In this section, we first describe the interaction Hamiltonian H_{I} in Eq. (6.11) of N indistinguishable laser-driven atomic particles inside a cavitating bubble. We then identify the relevant states and relevant coupling constants before discussing the proposed two-stage cooling process in some detail.

6.4.1 Basic idea

In analogy to the definition in Eq. (6.16), we denote the atomic state with all atoms in the ground state in the following by $|g\rangle$,

$$|g\rangle \quad = \quad |00\ldots0\rangle\,. \tag{6.53}$$

To see which excited state needs to be taken into account in the following discussion, we apply the laser term in the interaction Hamiltonian H_{I} in Eq. (6.11) of N to $|g\rangle$ and find that

$$\sum_{i=1}^{N} \frac{1}{2}\hbar\Omega\sigma_i^+ |g\rangle \quad = \quad \frac{1}{2}\hbar\sqrt{N}\Omega\,|s\rangle \tag{6.54}$$

with the highly symmetric atomic state $|s\rangle$ defined as

$$\begin{aligned} |s\rangle \quad = \quad & \frac{1}{\sqrt{N}}[|0\ldots01\rangle + |0\ldots010\rangle + \ldots \\ & +|010\ldots0\rangle + |10\ldots0\rangle]\,. \end{aligned} \tag{6.55}$$

To see which phonon mode is affected most strongly by the cooling laser, we now introduce the phonon operator

$$\langle s|H_{\mathrm{I}}|g\rangle \quad = \quad \frac{1}{2}\hbar\Omega\left[\sqrt{N} + \eta B_+^- + \eta' B_+^+\right] \tag{6.56}$$

with the collective phonon mode annihilation operator B_+ defined such that

$$B_+ \quad = \quad \frac{1}{\sqrt{N}}\sum_{i=1}^{N} b_i\,. \tag{6.57}$$

Similar to what we have seen in the previous section, this shows that the cooling laser removes energy effectively only from a single collective phonon mode. This collective phonon mode is symmetric with respect to exchanging the atomic particles and its annihilation operator obeys bosonic commutator relations due to the normalisation constant $\sqrt{N}$.

Introduce an effective Hamiltonian which is equivalent to a two-level system with a cooling laser. Taking into account Eq. (6.4.2) and having a closer look at the g-s subsystem dynamics, we find that this effective Hamiltonian equals

$$\begin{aligned} H_{\mathrm{eff}} \quad = \quad & \hbar\Delta\,|s\rangle\langle s| + \hbar(\nu + J)\,B_+^\dagger B_+ \\ & +\frac{1}{2}\hbar\Omega\left(\sqrt{N} + \eta B_+ + \eta' B_+^\dagger\right)\,|g\rangle\langle s| + \mathrm{H.c.} \end{aligned} \tag{6.58}$$

in analogy to Eq. (6.18). However, here we already neglected the terms which we know do not contribute to the cooling dynamics of the atoms. Moreover, we have seen in Section 6.2, that the spontaneous decay rate of the $|s\rangle$ state is N times as large as the spontaneous decay rate Γ of a single two-level atom.

Since N atomic particles have N independent phonon modes b_i, they also have N collective phonon mode operators which we denote B_i in the following and which are superpositions of the b_i operators such that they are all pairwise orthogonal. Collective phonon modes can be defined in many ways. Here we choose $B_1 = B_+$ and then define the remaining modes accordingly. Using this notation, the average mean phonon number per atom equals

$$m \;=\; \frac{1}{N}\sum_{i=1}^{N}\langle b_i^\dagger b_i\rangle \;=\; \frac{1}{N}\sum_{i=1}^{N}\langle B_i^\dagger B_i\rangle\,. \tag{6.59}$$

Here m is normalised such that it doesn't change significantly when atomic particles are removed or added to the trap. Notice that cooling the atoms to zero temperature is equivalent to reaching the point where $m = 0$. This applies in the presence and absence of collisions ($J \neq 0$).

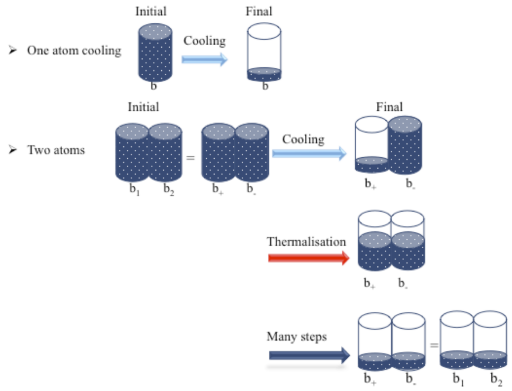

Figure 6.6: Diagrammatic representation of the dynamics of the sympathetic cooling process which consist of two stages :- thermalisation and cooling stages. there are two modes which are b_+ and b_- we can cool one of them to an even lower temperature and the final phonon number reaches the minimum value.

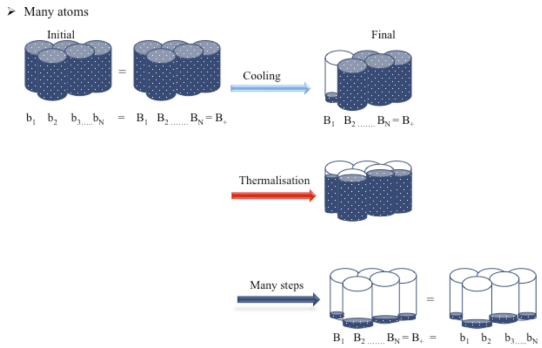

Figure 6.7: Diagrammatic representation of analytical model of the sympathetic cooling process which shows the final phonon numbers of many trapped atoms.

6.4.2 Cooling stages and thermalisation stages

In the previous section, we have seen that laser cooling can transfer a single collective phonon mode of the atoms to very low temperatures. When alternating cooling stages and thermalisation stages, we expect a constant transfer of vibrational energy from all phonon modes of the atoms into the single collective mode which is subsequently emptied during cooling stages. Eventually, this process will remove energy from all vibrational modes of the atoms. This is illustrated in Fig. 6.6 for the two-atom case and in Fig. 6.7 for the many atom case. Subsequent displacement stages transferred energy from all collective phonon modes into the B mode which can be cooled easily. Alternating both stages, the cooling process eventually resulted in the transfer of all vibrational modes of the strongly-confined atomic gas to very low phonon numbers.

Our two-step cooling scheme consists of cooling and thermalisation stages. The radius of the bubble which confines the atoms oscillates relatively rapidly. When it reaches its minimum radius, an optical cavity forms, cooling transitions become resonant and a cooling stage takes place. When the bubble radius is relatively large, the atoms do not see the cooling laser, they exchange energy via collisions and eventually thermalise. Here we refer to this stage as a thermalisation stage. Once the atomic gas inside the bubbles is cooled to very low temperatures, it could be used for sympathetic cooling of the surrounding liquid.

6.5 Summary

The many common characteristics between quantum optics experiments in cavitating bubbles with trapped ions and atoms suggest that the temperature can become very low. Cooling atoms may, for example, be applied in micro and nanotechnology in cavitating bubbles requiring very little volume cooling. We examined more deeply what the physical processes of the quantum heat exchanger are, and provide more guidance for quantum optics experiments with cavitating bubble (Aljaloud *et al.* (2020)). For simplicity, we assume that the bubbles are always transparent. This allowed us to derive cooling rates for the cooling of a single collective phonon mode during the collapse of the bubble. We also see that,

with the dynamics of the atoms between collapse phases, their thermal energy is efficiently redistributed.

We recently developed a model of a collective laser-cooling system to ensure that indistinguishable atoms of caviting bubbles can serve as the basic building blocks (Aljaloud *et al.* (2020)). In this chapter, we examined the physical processes underlying this study in greater detail and provide further guidance for quantum optics experiments with cavitating bubbles. For the sake of simplicity, the bubbles are always transparent. The case of atoms inside a cavitating bubble with cavity formation will be studied later.

Chapter 7

Conclusions

7.1 Overview

We have now arrived at the end of our investigation, and now we would like to organise everything we have learned throughout the project. In the present thesis, we have developed and analysed a quantum mechanical model of a multi-body atomic system for collective cooling and heating. In contrast to standard laser cooling which is a one-phase process, our model is a two-phase process, and uses quantum optical models in conjunction with the thermodynamic frameworks. The entire process is divided into thermalization, of multiple particles and the cooling phase, which reduces the temperature of a single collective phonon mode. Taking into account the symbiosis of these two steps, the collective dynamics of the multi-body atomic system are described appropriately. The quantum-optical cooling model is based on applying the master atomic system equation. In general, the system is expected to reach very low temperatures in alternating cooling and thermalisation stages.

In addition, our two-stage model takes advantage of the sonoluminescence mechanism. The bubble's collapse during sonoluminescence is accompanied by a period of growth of the bubble radius, and rapid increases in gas temperature inside the bubble. During the bubble expansion phase, the dynamics of the atomic gas inside the bubble can be described by the laws of thermodynamics. A rapid exchange of energy occurs between all phonon modes. During the bubble collapse phases and in the presence of a cooling laser, the system can be modelled by

quantum optics. The growth phase and the collapse of the bubble lifecycle result in naturally alternating thermalisation phases and cooling phases if a cooling laser is applied.

In chapter 5 we have highlighted similarities with strongly confined atomic particle experiments in quantum optics and single sonoluminescence bubble experiments. There are interactions in both situations, which can be used very efficiently to transform thermal energy into light. Therefore, we expect a quick transfer of heat to the light with the application of an external cooling laser to cavitating bubbles that may eventually lead to the cooling of small appliances. Our estimates show that cooling rates in the order of milliseconds for cubic micrometres of water may be reached by Kelvin temperature. Applications are expected in research testing and in micro and nanotechnology for the proposed quantum heat exchanger. There are already a wide range of applications in quantum technology, a closely related cooling process, namely the laser cooling of trapped ions. Our new findings and the general design of a quantum heat exchanger have been published in Aljaloud, Peyman and Beige (2020).

Chapter 6 provides a more detailed analysis of the proposed quantum heat exchanger (Aljaloud *et al.* (2020)). For simplicity, we assume here a bubble which does not become opaque during the collapse phase and no cavity is formed. Although optical cooling of solid-state systems is a very small volume operation, it immediately opens up a plethora of applications in quantum, nano, and microtechnology. We examined in greater detail the physical processes underlying this study and provide additional guidance for quantum optics experiments with cavitation bubbles. More concretely, we assumed that the bubbles are always transparent and that, in principle, atomic gas can be rapidly transferred to extremely low temperatures within a cavitating bubble. These conclusions will be published in Aljaloud and Beige (2021).

7.2 Future work

In the coming months, we plan to further analyse the proposed cooling scheme. For example, we still need to calculate a heat exchanger for bubbles with opaque walls as well as we can look at cavity cooling of indistinguishable particles in

cavitating bubbles in more detail. If the bubble forms an optical cavity, this might result in collectively enhanced cooling rates. In the longer term, we plan to introduce the role of entropy in the quantum thermodynamics of interacting atoms. We also plan to use our experience to develop a better understanding of sonoluminescence experiments. Potentially, these too can be controlled with laser interactions. Increasing the achievable temperatures in sonoluminescence experiments would have applications in sonofusion and sonochemistry.

References

Aljaloud, A., Peyman, S.A. & Beige, A. (2020). A quantum heat exchanger for nanotechnology. *Entropy*, **22**, 379. 72, 74, 82, 89, 98, 99, 101

Barber, B.P. & Putterman, S.J. (1991). Observation of synchronous picosecond sonoluminescence. *Nature*, **352**, 318–320. 21, 50, 52, 53

Barber, B.P. & Putterman, S.J. (1992). Light scattering measurements of the repetitive supersonic implosion of a sonoluminescing bubble. *Physical review letters*, **69**, 3839. 50

Barreiro, J.T., Müller, M., Schindler, P., Nigg, D., Monz, T., Chwalla, M., Hennrich, M., Roos, C.F., Zoller, P. & Blatt, R. (2011). An open-system quantum simulator with trapped ions. *Nature*, **470**, 486–491. 19, 71

Beige, A. & Kim, O. (2015a). A cavity-mediated collective quantum effect in sonoluminescing bubbles. In *Journal of Physics: Conference Series*, vol. 656, 012177, IOP Publishing. 57, 58, 63, 65, 70

Beige, A. & Kim, O. (2015b). A cavity-mediated collective quantum effect in sonoluminescing bubbles. *Journal of Physics: Conference Series*, **656**, 012177. 70

Beige, A., Knight, P.L. & Vitiello, G. (2005). Cooling many particles at once. *New Journal of Physics*, **7**, 96. 33, 36, 37, 38, 39, 63, 65

Bernstein, L.S. & Zakin, M.R. (1995). Confined electron model for single-bubble sonoluminescence. *The Journal of Physical Chemistry*, **99**, 14619–14627. 53

Blais, A., Girvin, S.M. & Oliver, W.D. (2020). Quantum information processing and quantum optics with circuit quantum electrodynamics. *Nature Physics*, **16**, 247–256. 41

Blaise, P. & Henri-Rousseau, O. (2011). *Quantum Oscillators*. John Wiley & Sons. 46

Blake, T., Kurcz, A. & Beige, A. (2011a). Comparing cavity and ordinary laser cooling within the lamb–dicke regime. *Journal of Modern Optics*, **58**, 1317–1328. 33, 34, 36, 38, 76, 78

Blake, T., Kurcz, A., Saleem, N.S. & Beige, A. (2011b). Laser cooling of a trapped particle with increased rabi frequencies. *Physical Review A*, **84**, 053416. 27, 29, 30, 36, 76, 78, 82

Blake, T., Kurcz, A. & Beige, A. (2012). Rate-equation approach to cavity-mediated laser cooling. *Physical Review A*, **86**, 013419. 33, 78

Brenner, M.P., Hilgenfeldt, S. & Lohse, D. (2002). Single-bubble sonoluminescence. *Reviews of modern physics*, **74**, 425. 21, 50, 52, 54, 56, 64, 65

Burdin, F., Tsochatzidis, N., Guiraud, P., Wilhelm, A. & Delmas, H. (1999). Characterisation of the acoustic cavitation cloud by two laser techniques. *Ultrasonics Sonochemistry*, **6**, 43–51. 50

Camara, C., Putterman, S. & Kirilov, E. (2004). Sonoluminescence from a single bubble driven at 1 megahertz. *Physical review letters*, **92**, 124301. 21, 50, 52, 53, 56, 64, 65

Cao, G., Danworaphong, S. & Diebold, G.J. (2008). A search for laser heating of a sonoluminescing bubble. *The European Physical Journal Special Topics*, **153**, 215–221. 63

Chu, S. (1998). Nobel lecture: The manipulation of neutral particles. *Reviews of Modern Physics*, **70**, 685. 19, 26

Chuah, B.L., Lewty, N.C., Cazan, R. & Barrett, M.D. (2013). Sub-doppler cavity cooling beyond the lamb-dicke regime. *Physical Review A*, **87**, 043420. 32

Ciawi, E., Rae, J., Ashokkumar, M. & Grieser, F. (2006). Determination of temperatures within acoustically generated bubbles in aqueous solutions at different ultrasound frequencies. *The Journal of Physical Chemistry B*, **110**, 13656–13660. 50

Cirac, J., Parkins, A., Blatt, R. & Zoller, P. (1993). Cooling of a trapped ion coupled strongly to a quantized cavity mode. *Optics communications*, **97**, 353–359. 32, 36, 38

Cirac, J., Lewenstein, M. & Zoller, P. (1995). Laser cooling a trapped atom in a cavity: Bad-cavity limit. *Physical Review A*, **51**, 1650. 33, 36, 38

Cohen-Tannoudji, C.N. (1998). Nobel lecture: Manipulating atoms with photons. *Reviews of Modern Physics*, **70**, 707. 26

Cohen-Tannoudji, C.N. & Phillips, W.D. (1990). New mechanisms for laser cooling. *Phys. Today*, **43**, 33–40. 26

Cornell, E.A. & Wieman, C.E. (2002). Bose–einstein condensation in a dilute gas: the first 70 years and some recent experiments (nobel lecture). *Chemphyschem*, **3**, 476–493. 25

Daul, J.M. & Grangier, P. (2005a). Cavity-induced damping and level shifts in a wide aperture spherical resonator. *The European Physical Journal D-Atomic, Molecular, Optical and Plasma Physics*, **32**, 181–194. 63

Daul, J.M. & Grangier, P. (2005b). Vacuum-field atom trapping in a wide aperture spherical resonator. *The European Physical Journal D-Atomic, Molecular, Optical and Plasma Physics*, **32**, 195–200. 63

Debnath, S., Linke, N.M., Figgatt, C., Landsman, K.A., Wright, K. & Monroe, C. (2016). Demonstration of a small programmable quantum computer with atomic qubits. *Nature*, **536**, 63–66. 19, 71

Didenko, Y.T. & Gordeychuk, T. (2000). Multibubble sonoluminescence spectra of water which resemble single-bubble sonoluminescence. *Physical review letters*, **84**, 5640. 52, 53

Didenko, Y.T., McNamara III, W.B. & Suslick, K.S. (2000). Effect of noble gases on sonoluminescence temperatures during multibubble cavitation. *Physical review letters*, **84**, 777. 21, 52

Diedrich, F., Bergquist, J., Itano, W.M. & Wineland, D. (1989). Laser cooling to the zero-point energy of motion. *Physical Review Letters*, **62**, 403. 31

DiVincenzo, D.P. (1995). Quantum computation. *Science*, **270**, 255–261. 25

Domokos, P. & Ritsch, H. (2002). Collective cooling and self-organization of atoms in a cavity. *Physical review letters*, **89**, 253003. 20, 63

Domokos, P. & Ritsch, H. (2003). Mechanical effects of light in optical resonators. *JOSA B*, **20**, 1098–1130. 32, 33

Eddingsaas, N.C. & Suslick, K.S. (2007). Evidence for a plasma core during multibubble sonoluminescence in sulfuric acid. *Journal of the American Chemical Society*, **129**, 3838–3839. 50, 52, 54

Flannigan, D.J. & Suslick, K.S. (2005). Plasma formation and temperature measurement during single-bubble cavitation. *Nature*, **434**, 52–55. 14, 50, 52, 54, 57, 59, 60, 64, 65

Flannigan, D.J. & Suslick, K.S. (2006). Plasma quenching by air during single-bubble sonoluminescence. *The Journal of Physical Chemistry A*, **110**, 9315–9318. 50, 52

Flannigan, D.J. & Suslick, K.S. (2007). Emission from electronically excited metal atoms during single-bubble sonoluminescence. *Physical review letters*, **99**, 134301. 21, 50, 52, 54

Flannigan, D.J., Hopkins, S.D. & Suslick, K.S. (2005). Sonochemistry and sonoluminescence in ionic liquids, molten salts, and concentrated electrolyte solutions. *Journal of Organometallic Chemistry*, **690**, 3513–3517. 19, 56, 64, 65

Flint, E.B. & Suslick, K.S. (1991). The temperature of cavitation. *Science*, **253**, 1397–1399. 50

Frenzel, H. & Schultes, H. (1934). Luminescenz im ultraschallbeschickten wasser. *Zeitschrift für Physikalische Chemie*, **27**, 421–424. 49, 50

Frommhold, L. (1998). Electron-atom bremsstrahlung and the sonoluminescence of rare gas bubbles. *Physical Review E*, **58**, 1899. 53

Frommhold, L. & Atchley, A.A. (1994). Is sonoluminescence due to collision-induced emission? *Physical review letters*, **73**, 2883. 53

Gaitan, D. & Crum, L. (1990a). Observation of sonoluminescence from a single, stable cavitation bubble in a water/glycerine mixture. frontiers of nonlinear acoustics. 12th isna. *12th ISNA*, 459. 50

Gaitan, D.F. & Crum, L.A. (1990b). Sonoluminescence from single bubbles. *The Journal of the Acoustical Society of America*, **87**, S141–S141. 50

Gaitan, D.F., Crum, L.A., Church, C.C. & Roy, R.A. (1992). Sonoluminescence and bubble dynamics for a single, stable, cavitation bubble. *The Journal of the Acoustical Society of America*, **91**, 3166–3183. 21, 49, 50, 56, 64, 65

Garcia, N. & Levanyuk, A. (1996). Sonoluminescence: A new electrical breakdown hypothesis. *Journal of Experimental and Theoretical Physics Letters*, **64**, 907–910. 53

Gerry, C., Knight, P. & Knight, P.L. (2005). *Introductory quantum optics*. Cambridge university press. 40

Gompf, B., Günther, R., Nick, G., Pecha, R. & Eisenmenger, W. (1997). Resolving sonoluminescence pulse width with time-correlated single photon counting. *Physical Review Letters*, **79**, 1405. 52

Goodwin, J.F., Stutter, G., Thompson, R.C. & Segal, D.M. (2016). Resolved-sideband laser cooling in a penning trap. *Physical review letters*, **116**, 143002. 27

Hänsch, T.W. & Schawlow, A.L. (1975). Cooling of gases by laser radiation. *Optics Communications*, **13**, 68–69. 19, 26, 72

Haroche, S. & Raimond, J.M. (2006). *Exploring the quantum: atoms, cavities, and photons*. Oxford university press. 40

Hemmerling, M. & Robb, G. (2011). Cavity cooling using intense blue-detuned light. *Journal of Modern Optics*, **58**, 1336–1341. 32

Hilgenfeldt, S., Lohse, D. & Moss, W.C. (1998). Water temperature dependence of single bubble sonoluminescence. *Physical review letters*, **80**, 1332. 50

Hilgenfeldt, S., Grossmann, S. & Lohse, D. (1999a). A simple explanation of light emission in sonoluminescence. *Nature*, **398**, 402–405. 53

Hilgenfeldt, S., Grossmann, S. & Lohse, D. (1999b). Sonoluminescence light emission. *Physics of fluids*, **11**, 1318–1330. 53

Hilgenfeldt, S., Lohse, D. & Zomack, M. (2000). Sound scattering and localized heat deposition of pulse-driven microbubbles. *The Journal of the Acoustical Society of America*, **107**, 3530–3539. 50

Hiller, R., Putterman, S.J. & Barber, B.P. (1992). Spectrum of synchronous picosecond sonoluminescence. *Physical Review Letters*, **69**, 1182. 50, 52, 53

Hiller, R., Weninger, K., Putterman, S.J. & Barber, B.P. (1994). Effect of noble gas doping in single-bubble sonoluminescence. *Science*, **266**, 248–250. 50

Hiller, R.A., Putterman, S.J. & Weninger, K.R. (1998). Time-resolved spectra of sonoluminescence. *Physical Review Letters*, **80**, 1090. 50, 52, 53

Hopkins, S.D., Putterman, S.J., Kappus, B.A., Suslick, K.S. & Camara, C.G. (2005). Dynamics of a sonoluminescing bubble in sulfuric acid. *Physical review letters*, **95**, 254301. 53

Hsu, T.R. (2008). *MEMS and microsystems: design, manufacture, and nanoscale engineering*. John Wiley & Sons. 62

Kampschulte, T., Alt, W., Brakhane, S., Eckstein, M., Reimann, R., Widera, A. & Meschede, D. (2010). Optical control of the refractive index of a single atom. *Physical review letters*, **105**, 153603. 32

Ketterle, W. & Van Druten, N. (1996). Evaporative cooling of trapped atoms. *Advances in atomic, molecular, and optical physics*, **37**, 181–236. 26

Khalid, S., Kappus, B., Weninger, K. & Putterman, S. (2012). Opacity and transport measurements reveal that dilute plasma models of sonoluminescence are not valid. *Physical review letters*, **108**, 104302. 58, 63

Kim, O. & Beige, A. (2013). Mollow triplet for cavity-mediated laser cooling. *Physical Review A*, **88**, 053417. 34, 36, 38

Kim, O., Deb, P. & Beige, A. (2018). Cavity-mediated collective laser-cooling of a non-interacting atomic gas inside an asymmetric trap to very low temperatures. *Journal of Modern Optics*, **65**, 693–705. 18, 34, 36, 38, 39, 63, 65

Kim, P., Shi, L., Majumdar, A. & McEuen, P.L. (2001). Thermal transport measurements of individual multiwalled nanotubes. *Physical review letters*, **87**, 215502. 63

Kurcz, A., Capolupo, A. & Beige, A. (2009a). Quantum optical heating in sonoluminescence experiments. In *AIP Conference Proceedings*, vol. 1114, 31–36, American Institute of Physics. 54

Kurcz, A., Capolupo, A. & Beige, A. (2009b). Sonoluminescence and quantum optical heating. *New Journal of Physics*, **11**, 053001. 54, 57, 58, 63, 65, 70

Lauterborn, W. & Koch, A. (1987). Holographic observation of period-doubled and chaotic bubble oscillations in acoustic cavitation. *Physical Review A*, **35**, 1974. 50

Lee, J., Ashokkumar, M., Kentish, S. & Grieser, F. (2005). Determination of the size distribution of sonoluminescence bubbles in a pulsed acoustic field. *Journal of the American Chemical Society*, **127**, 16810–16811. 50

Leibfried, D., Blatt, R., Monroe, C. & Wineland, D. (2003a). Quantum dynamics of single trapped ions. *Reviews of Modern Physics*, **75**, 281. 19, 54

Leibfried, D., DeMarco, B., Meyer, V., Lucas, D., Barrett, M., Britton, J., Itano, W.M., Jelenković, B., Langer, C., Rosenband, T. *et al.* (2003b). Experimental demonstration of a robust, high-fidelity geometric two ion-qubit phase gate. *Nature*, **422**, 412–415. 19, 71

Lev, B.L., Vukics, A., Hudson, E.R., Sawyer, B.C., Domokos, P., Ritsch, H. & Ye, J. (2008). Prospects for the cavity-assisted laser cooling of molecules. *Physical Review A*, **77**, 023402. 31

Lohse, D. (2002). Inside a micro-reactor. *Nature*, **418**, 381–383. 21

Loudon, R. (2000). *The quantum theory of light*. OUP Oxford. 41

Ludlow, A.D., Boyd, M.M., Ye, J., Peik, E. & Schmidt, P.O. (2015). Optical atomic clocks. *Reviews of Modern Physics*, **87**, 637. 19, 71

Madison, K.W. (2013). Annual review of cold atoms and molecules. 20

Maiwald, R., Leibfried, D., Britton, J., Bergquist, J.C., Leuchs, G. & Wineland, D.J. (2009). Stylus ion trap for enhanced access and sensing. *Nature Physics*, **5**, 551–554. 19, 71

Maunz, P., Puppe, T., Schuster, I., Syassen, N., Pinkse, P.W. & Rempe, G. (2004). Cavity cooling of a single atom. *Nature*, **428**, 50–52. 20, 32

McKeever, J., Buck, J., Boozer, A., Kuzmich, A., Nägerl, H.C., Stamper-Kurn, D. & Kimble, H. (2003). State-insensitive cooling and trapping of single atoms in an optical cavity. *Physical review letters*, **90**, 133602. 20, 32

McNamara, W.B., Didenko, Y.T. & Suslick, K.S. (1999). Sonoluminescence temperatures during multi-bubble cavitation. *nature*, **401**, 772–775. 49

Moss, W.C. (1997). Understanding the periodic driving pressure in the rayleigh–plesset equation. *The Journal of the Acoustical Society of America*, **101**, 1187–1190. 51, 53, 57, 63

Moss, W.C., Clarke, D.B., White, J.W. & Young, D.A. (1994). Hydrodynamic simulations of bubble collapse and picosecond sonoluminescence. *Physics of Fluids*, **6**, 2979–2985. 53

Moss, W.C., Young, D.A., Harte, J.A., Levatin, J.L., Rozsnyai, B.F., Zimmerman, G.B. & Zimmerman, I.H. (1999). Computed optical emissions from a sonoluminescing bubble. *Physical Review E*, **59**, 2986. 53

Mossberg, T., Lewenstein, M. & Gauthier, D.J. (1991). Trapping and cooling of atoms in a vacuum perturbed in a frequency-dependent manner. *Physical review letters*, **67**, 1723. 32

Murr, K. (2006). Large velocity capture range and low temperatures with cavities. *Physical review letters*, **96**, 253001. 32

Neuhauser, W., Hohenstatt, M., Toschek, P. & Dehmelt, H. (1978). Optical-sideband cooling of visible atom cloud confined in parabolic well. *Physical Review Letters*, **41**, 233. 19

Nussmann, S., Murr, K., Hijlkema, M., Weber, B., Kuhn, A. & Rempe, G. (2005). Vacuum-stimulated cooling of single atoms in three dimensions. *Nature Physics*, **1**, 122–125. 20, 32

Ohl, C.D., Lindau, O. & Lauterborn, W. (1998). Luminescence from spherically and aspherically collapsing laser induced bubbles. *Physical Review Letters*, **80**, 393. 50

Phillips, W.D. (1998). Nobel lecture: Laser cooling and trapping of neutral atoms. *Reviews of Modern Physics*, **70**, 721. 19, 26

Phillips, W.D. & Metcalf, H. (1982). Laser deceleration of an atomic beam. *Physical Review Letters*, **48**, 596.

Planck, M. (1901). On the law of the energy distribution in the normal spectrum. *Ann. Phys*, **4**, 1–11. 41

Porras, D. & Cirac, J.I. (2004). Effective quantum spin systems with trapped ions. *Physical review letters*, **92**, 207901. 19, 71

Putterman, S., Evans, P., Vazquez, G. & Weninger, K. (2001). Is there a simple theory of sonoluminescence? *Nature*, **409**, 782–783. 21

Rae, J., Ashokkumar, M., Eulaerts, O., von Sonntag, C., Reisse, J. & Grieser, F. (2005). Estimation of ultrasound induced cavitation bubble temperatures in aqueous solutions. *Ultrasonics sonochemistry*, **12**, 325–329. 50

Ritsch, H., Domokos, P., Brennecke, F. & Esslinger, T. (2013). Cold atoms in cavity-generated dynamical optical potentials. *Reviews of Modern Physics*, **85**, 553. 63

Saniei, N. (2007). Nanotechnology and heat transfer. *Heat transfer engineering*, **28**, 255–257. 63

Schleier-Smith, M.H., Leroux, I.D., Zhang, H., Van Camp, M.A. & Vuletić, V. (2011). Optomechanical cavity cooling of an atomic ensemble. *Physical review letters*, **107**, 143005. 33

Schmidt-Kaler, F., Häffner, H., Riebe, M., Gulde, S., Lancaster, G.P., Deuschle, T., Becher, C., Roos, C.F., Eschner, J. & Blatt, R. (2003). Realization of the cirac–zoller controlled-not quantum gate. *Nature*, **422**, 408–411. 19, 71

Schwinger, J. (1992). Casimir energy for dielectrics: spherical geometry. *Proceedings of the National Academy of Sciences of the United States of America*, **89**, 11118. 53

Stenholm, S. (1986). The semiclassical theory of laser cooling. *Reviews of modern physics*, **58**, 699. 27, 29, 36

Stephenson, L., Nadlinger, D., Nichol, B., An, S., Drmota, P., Ballance, T., Thirumalai, K., Goodwin, J., Lucas, D. & Ballance, C. (2020). High-rate, high-fidelity entanglement of qubits across an elementary quantum network. *Physical review letters*, **124**, 110501. 19, 71

Stick, D., Hensinger, W., Olmschenk, S., Madsen, M., Schwab, K. & Monroe, C. (2006). Ion trap in a semiconductor chip. *Nature Physics*, **2**, 36–39. 27

Suslick, K.S. (1990). Sonochemistry. *science*, **247**, 1439–1445. 64

Suslick, K.S. & Flannigan, D.J. (2008). Inside a collapsing bubble: sonoluminescence and the conditions during cavitation. *Annu. Rev. Phys. Chem.*, **59**, 659–683. 14, 21, 50, 52, 54, 57, 59, 60

Tsochatzidis, N., Guiraud, P., Wilhelm, A. & Delmas, H. (2001). Determination of velocity, size and concentration of ultrasonic cavitation bubbles by the phase-doppler technique. *Chemical engineering science*, **56**, 1831–1840. 50

Uruñuela, E., Alt, W., Keiler, E., Meschede, D., Pandey, D., Pfeifer, H. & Macha, T. (2020). Ground-state cooling of a single atom inside a high-bandwidth cavity. *Physical Review A*, **101**, 023415. 36, 38

Vazquez, G., Camara, C., Putterman, S. & Weninger, K. (2001). Sonoluminescence: nature's smallest blackbody. *Optics letters*, **26**, 575–577. 50, 52, 53

Vazquez, G., Camara, C., Putterman, S. & Weninger, K. (2002). Blackbody spectra for sonoluminescing hydrogen bubbles. *Physical review letters*, **88**, 197402. 50, 52, 53

Vigneron, K. (1995). Etude d'effets de bistabilite optique induits par des atomes froids places dans une cavite optique. *Stage de fin d'étude Supoptique*. 20, 32

Vuletić, V. & Chu, S. (2000). Laser cooling of atoms, ions, or molecules by coherent scattering. *Physical Review Letters*, **84**, 3787. 32

Walton, A.J. & Reynolds, G.T. (1984). Sonoluminescence. *Advances in physics*, **33**, 595–660. 49, 50

Willison, J.R. (1998). Sonoluminescence: proton-tunneling radiation. *Physical review letters*, **81**, 5430. 53

Wineland, D. & Dehmelt, H. (1975). Proposed $1014\delta\nu/\nu$ laser fluorescence spectroscopy on tl+ mono-ion oscillator iii (side band cooling). *Bull. Am. Phys. Soc*, **20**, 637–637. 19, 26, 72

Wineland, D.J. & Itano, W.M. (1979). Laser cooling of atoms. *Physical Review A*, **20**, 1521. 72

Wineland, D.J., Drullinger, R.E. & Walls, F.L. (1978). Radiation-pressure cooling of bound resonant absorbers. *Physical Review Letters*, **40**, 1639. 19

Wolke, M., Klinner, J., Kessler, H. & Hemmerich, A. (2012). Cavity cooling below the recoil limit. *Science*, **337**, 75–78. 32

Wu, C. & Roberts, P.H. (1993). Shock-wave propagation in a sonoluminescing gas bubble. *Physical review letters*, **70**, 3424. 53

Xu, N., Wang, L. & Hu, X. (1998). Numerical study of electronic impact and radiation in sonoluminescence. *Physical Review E*, **57**, 1615. 53

Zaugg, T., Wilkens, M., Meystre, P. & Lenz, G. (1993). Adiabatic atomic cooling in microwave cavities. *Optics communications*, **97**, 189–193. 32